INAF

ISTITUTO NAZIONALE DI ASTROFISICA
OSSERVATORIO ASTROFISICO DI ARCETRI

UNIVERSITÀ DEGLI STUDI FIRENZE

Lecture III:
The Spectral Energy Distribution of Galaxies
The optical spectrum of starlight

Astrophysics of Galaxies 2019-2020

Stefano Zibetti - INAF Osservatorio Astrofisico di Arcetri

Spectral Energy Distribution(s)

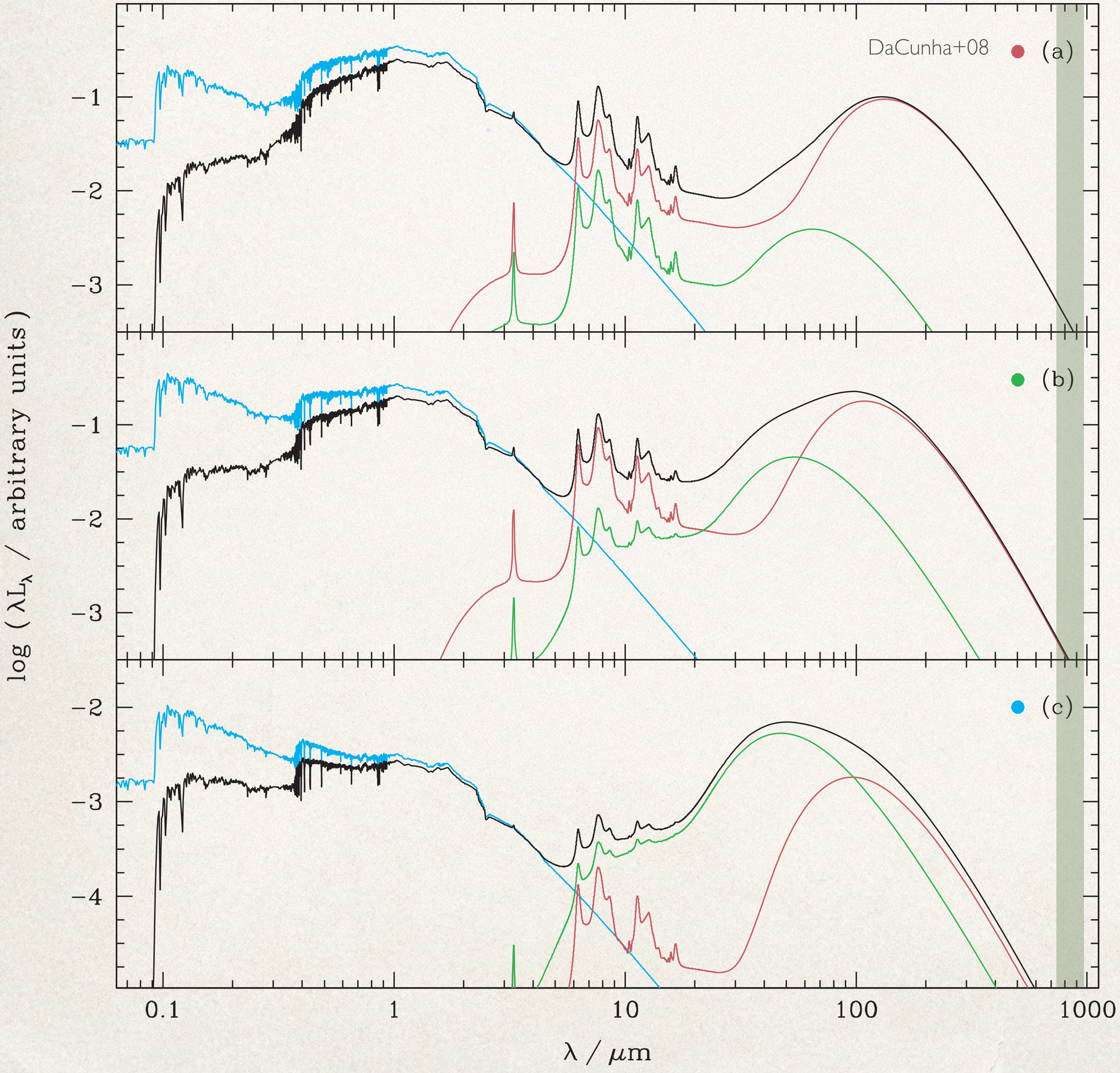

- Specific Luminosity as a function of wavelength or frequency
- Why $\log(\lambda f_\lambda)$?

$$F_{dex} \equiv \log\left(\int_{\lambda_0}^{10\lambda_0} d\lambda\, f_\lambda\right) = \log\left(\langle f_\lambda \rangle \cdot 9\lambda_0\right) =$$
$$= k + \log\left(\langle \lambda \rangle \cdot \langle f_\lambda \rangle\right)$$

Spectral Energy Distribution(s)

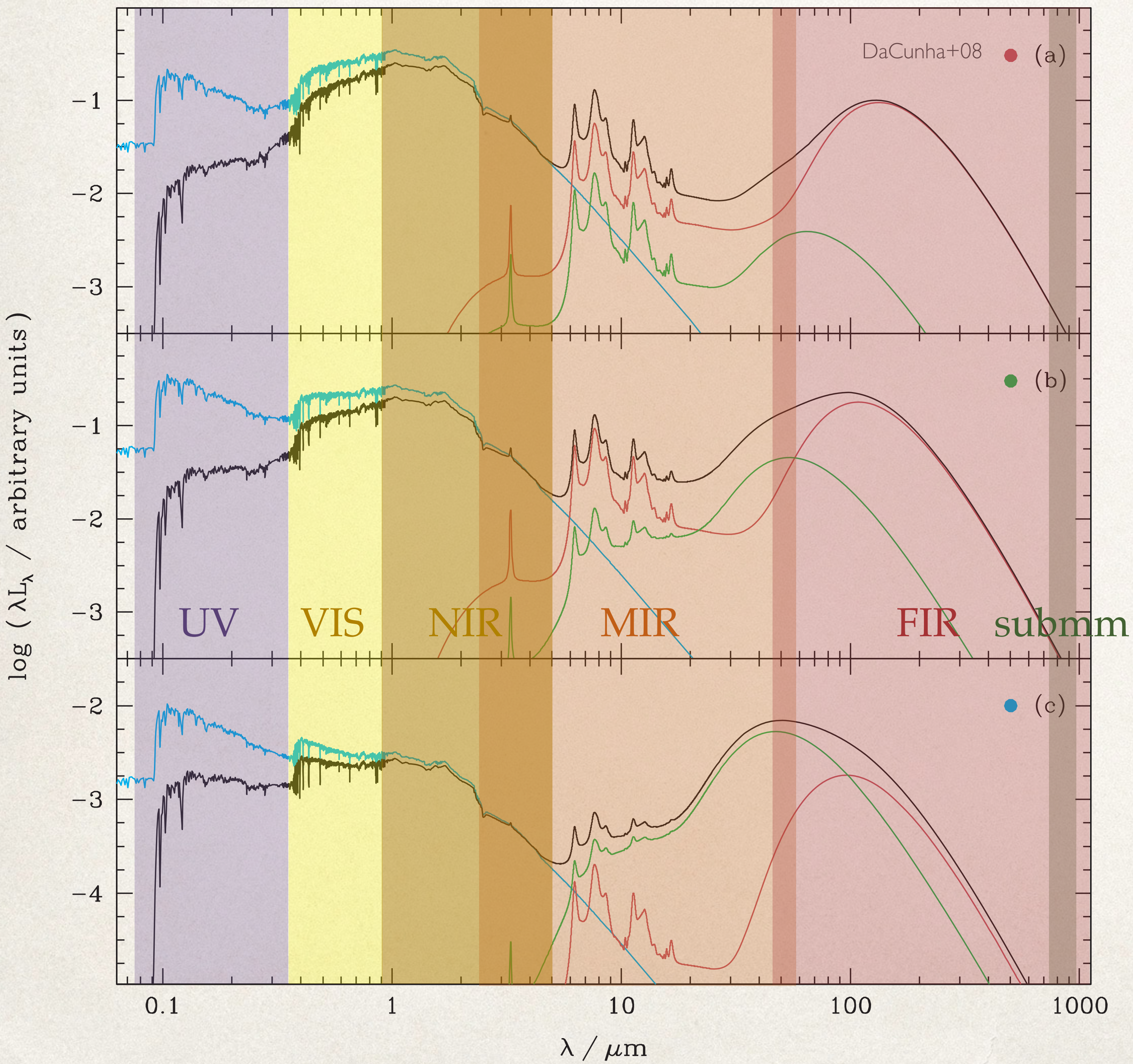

- Specific Luminosity as a function of wavelength or frequency
- Why $\log(\lambda f_\lambda)$?

$$F_{dex} \equiv \log\left(\int_{\lambda_0}^{10\lambda_0} d\lambda\, f_\lambda\right) = \log(<f_\lambda>\cdot 9\lambda_0) =$$
$$= k + \log(<\lambda>\cdot<f_\lambda>)$$

Spectral Energy Distribution(s)

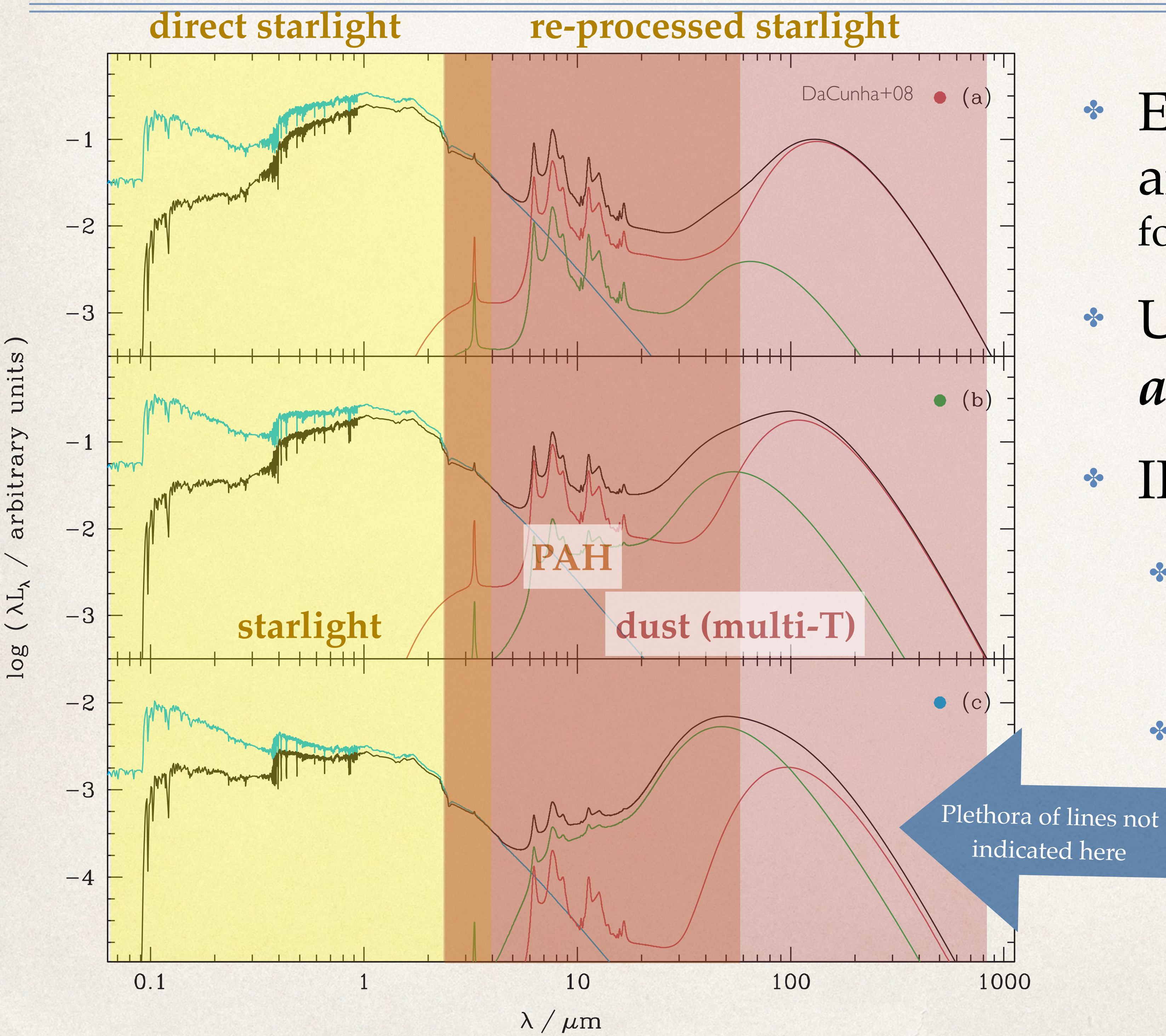

- Emission powered by stars and starlight (neglect black holes for the moment)
- UV-VIS-NIR: direct or ***dust-attenuated*** starlight
- IR (mainly MIR+FIR)
  - re-emission by dust as pseudo-blackbody
  - re-emission by molecules, simple (CO, H_2…) and complex (PAH)

Spectral Energy Distribution(s)

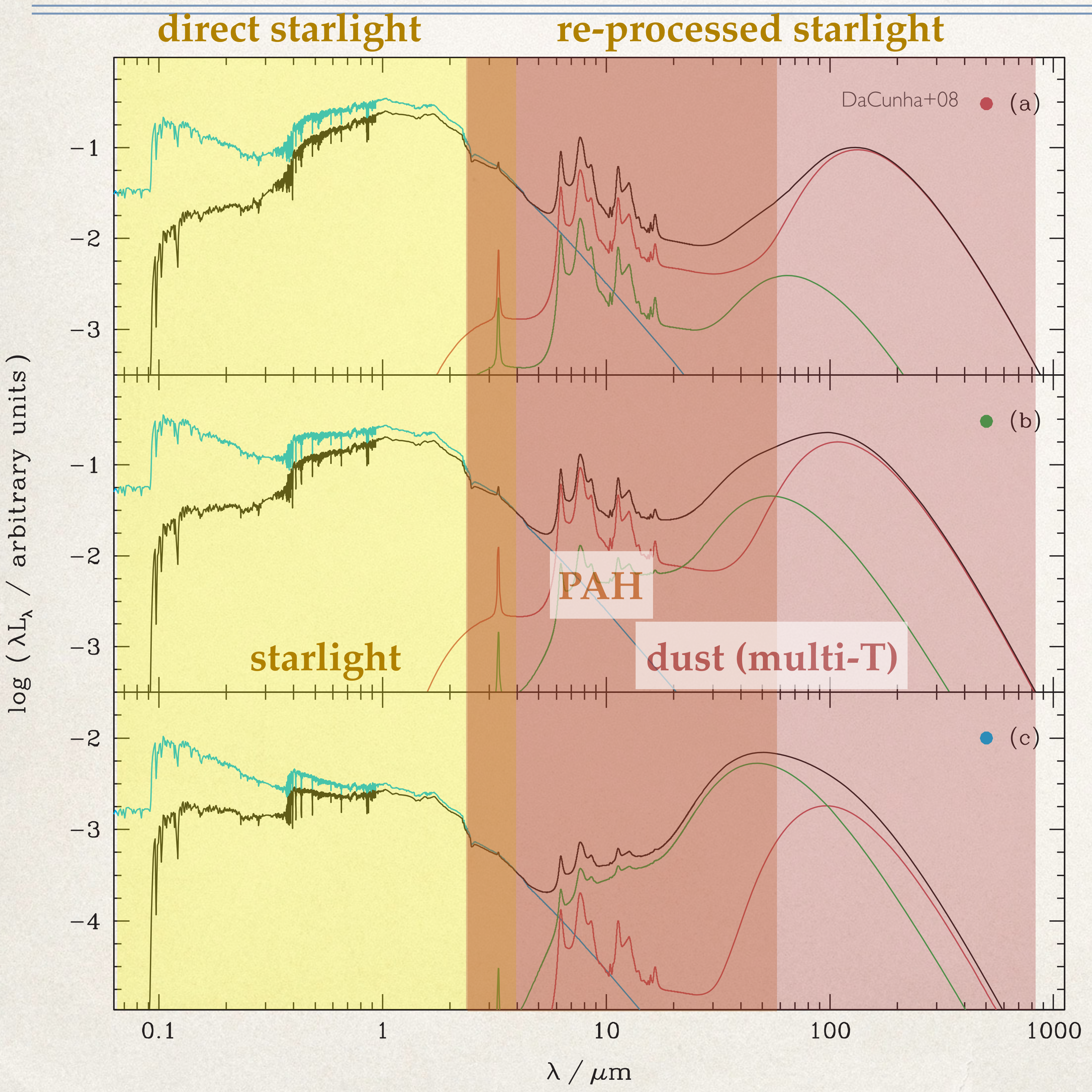

Note

Spectral Energy Distribution(s)

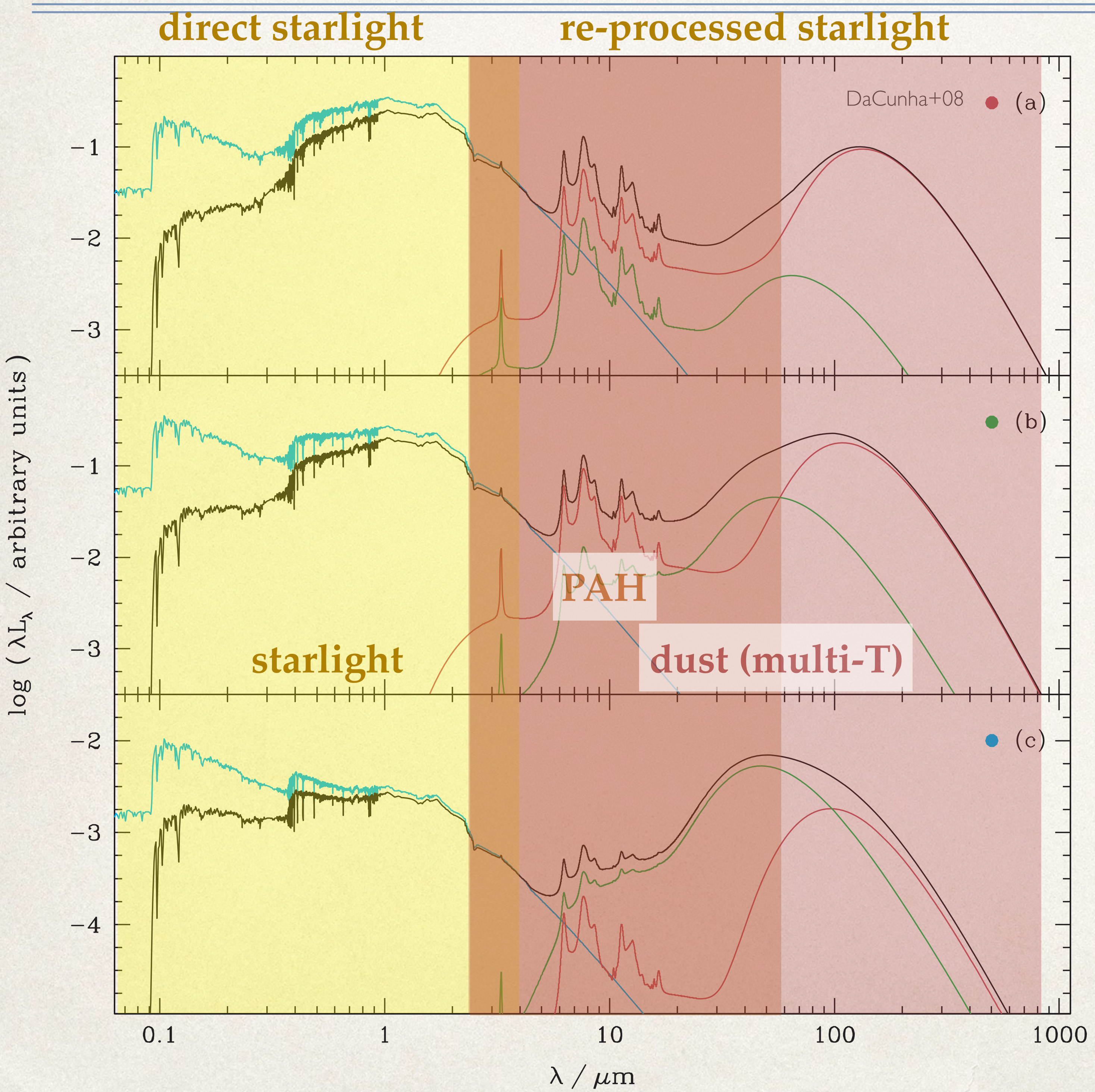

Note

- the different shape of the stellar continuum

Spectral Energy Distribution(s)

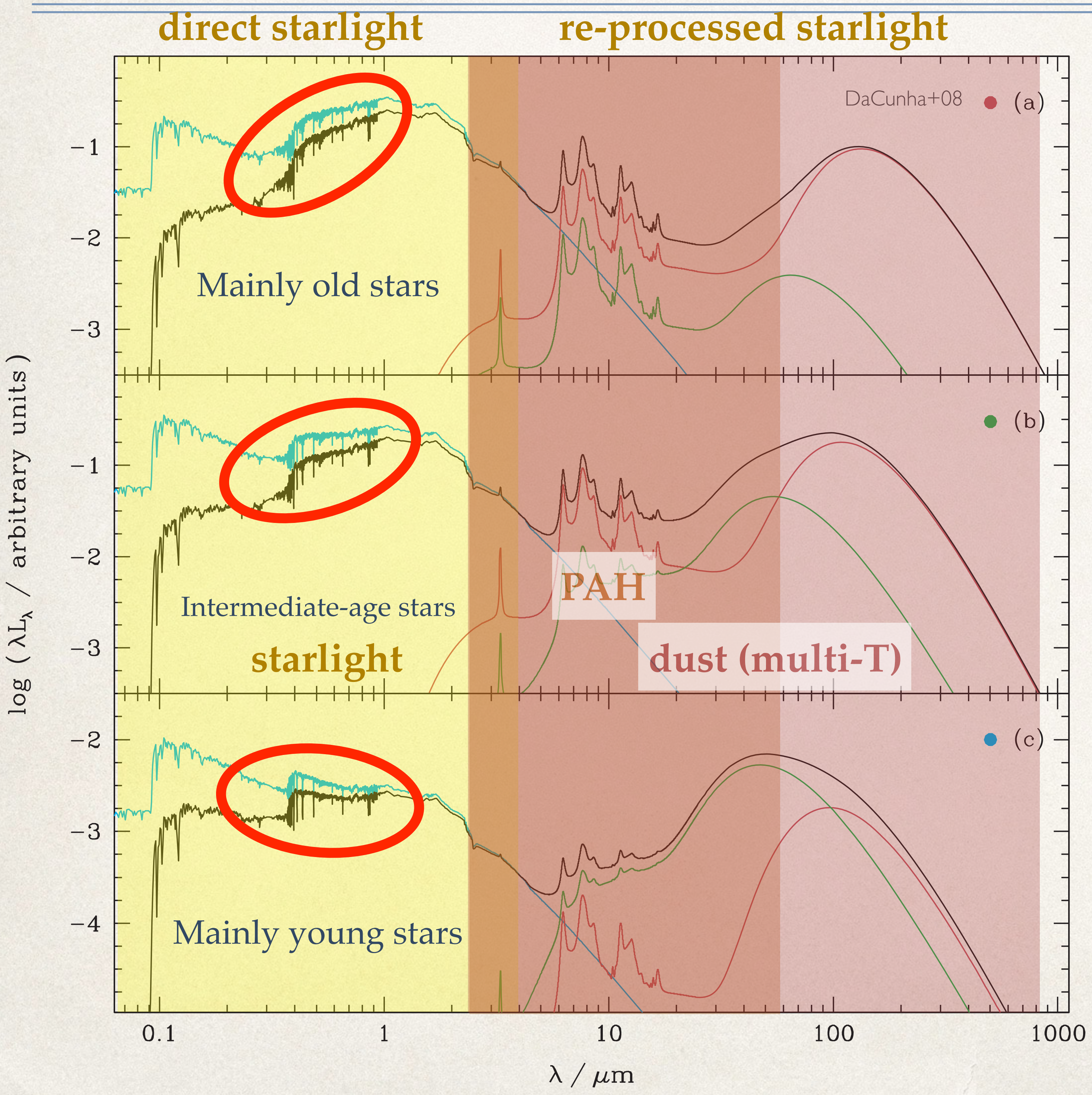

Note

- the different shape of the stellar continuum
  - emitted

Spectral Energy Distribution(s)

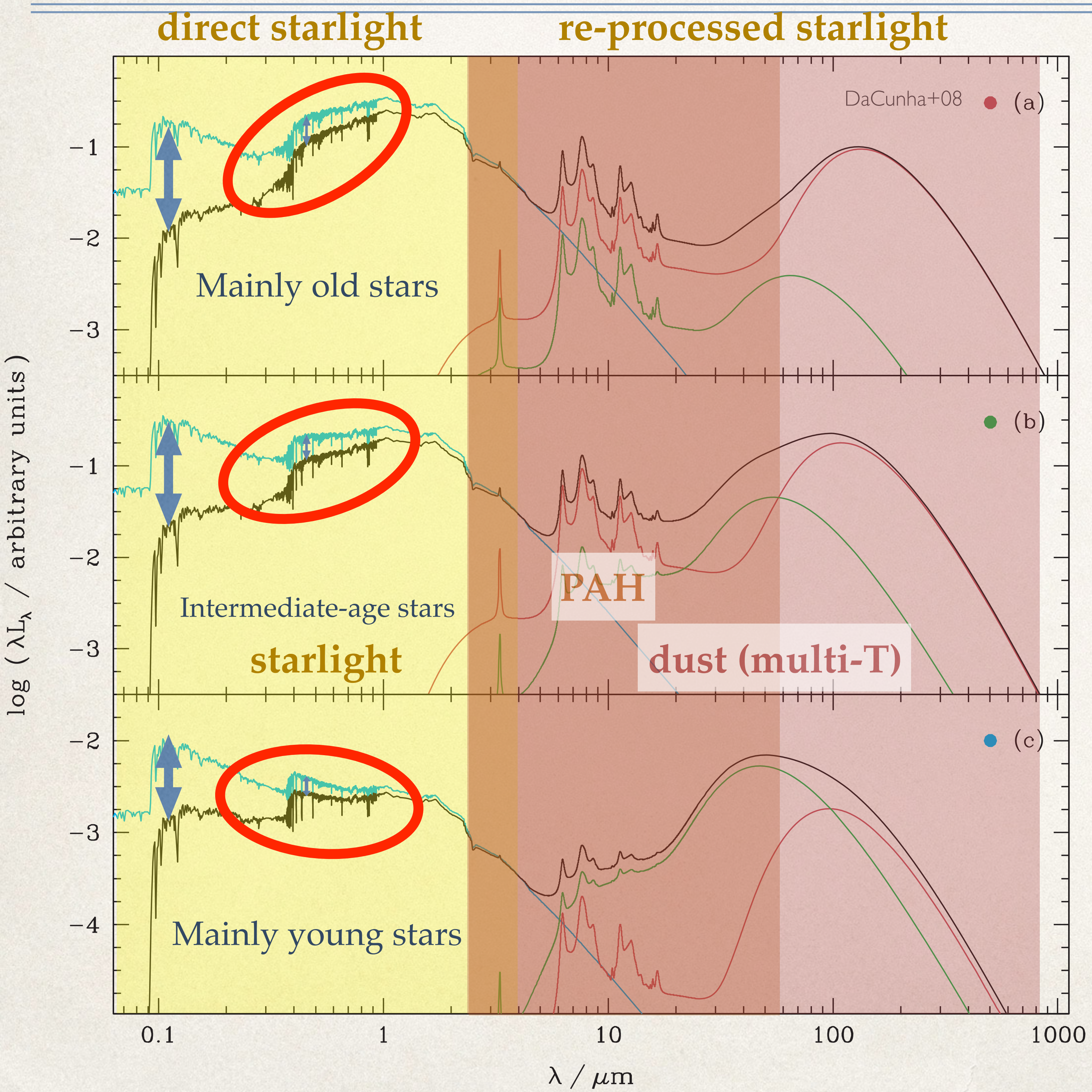

Note

- the different shape of the stellar continuum
  - emitted
  - attenuated (note dependence on λ)

Spectral Energy Distribution(s)

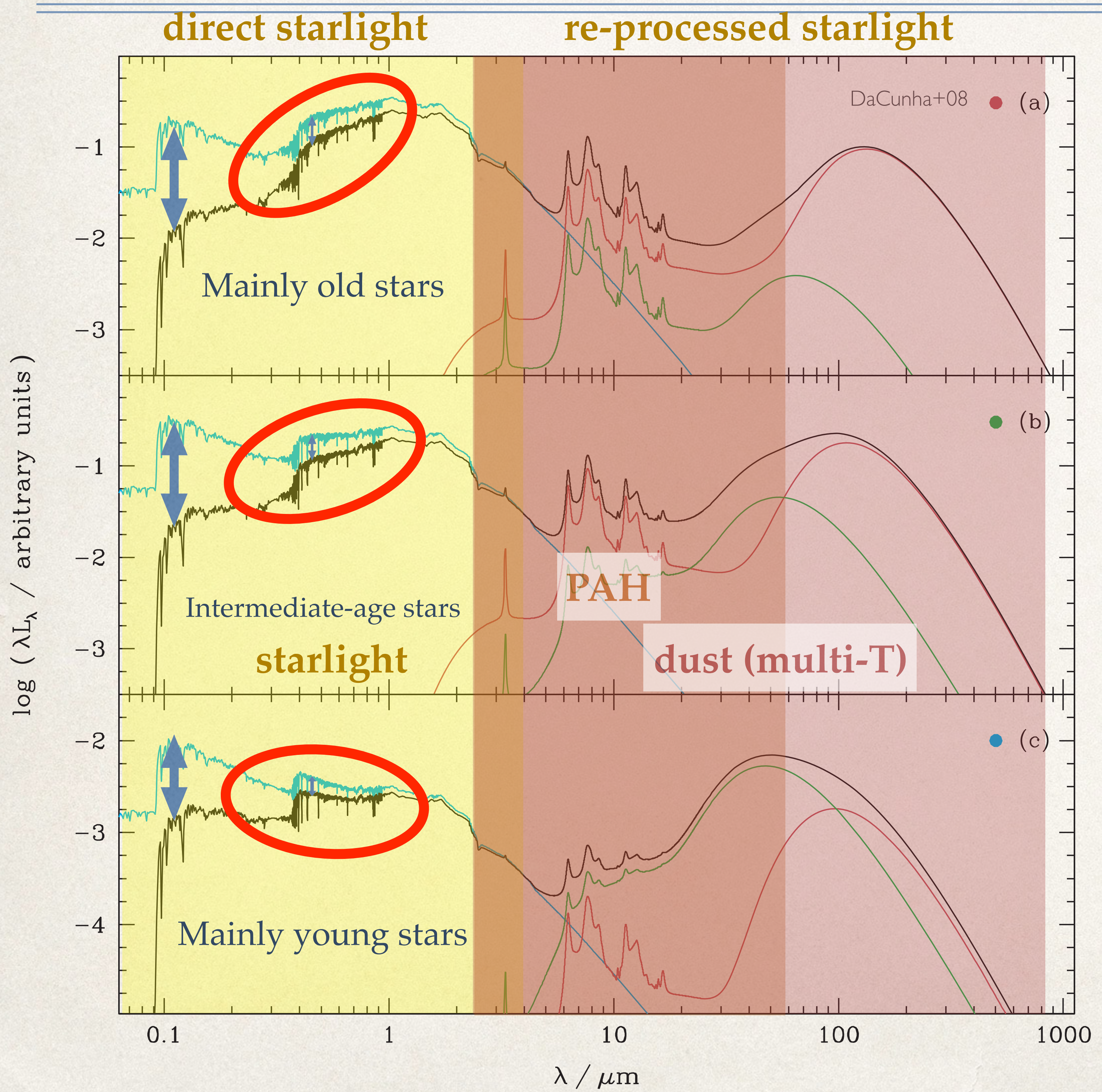

Note

- the different shape of the stellar continuum
  - emitted
  - attenuated (note dependence on λ)
- the corresponding shift of the dust emission

Spectral Energy Distribution(s)

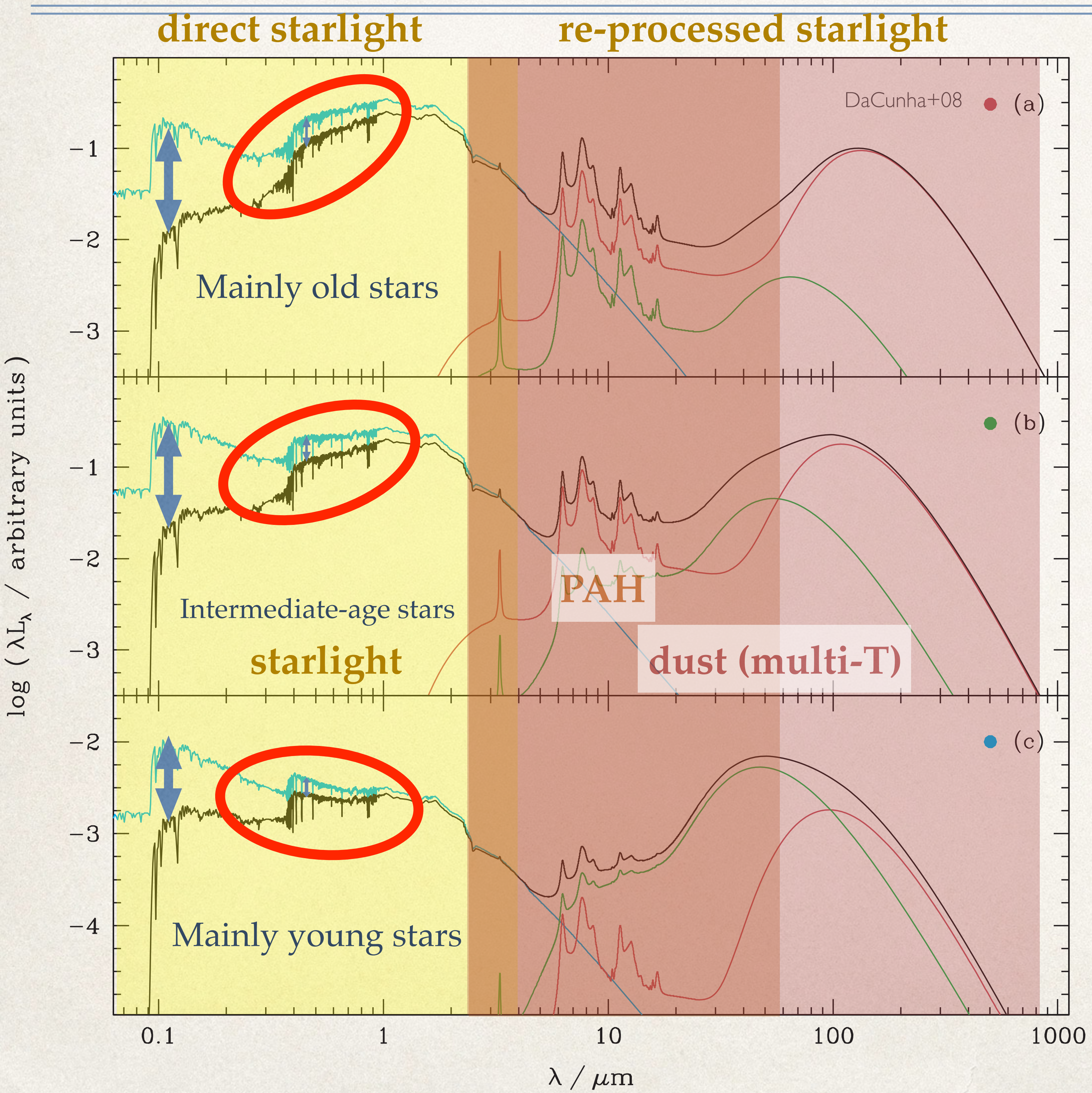

Note

- the different shape of the stellar continuum
  - emitted
  - attenuated (note dependence on λ)
- the corresponding shift of the dust emission
  - in Luminosity

Spectral Energy Distribution(s)

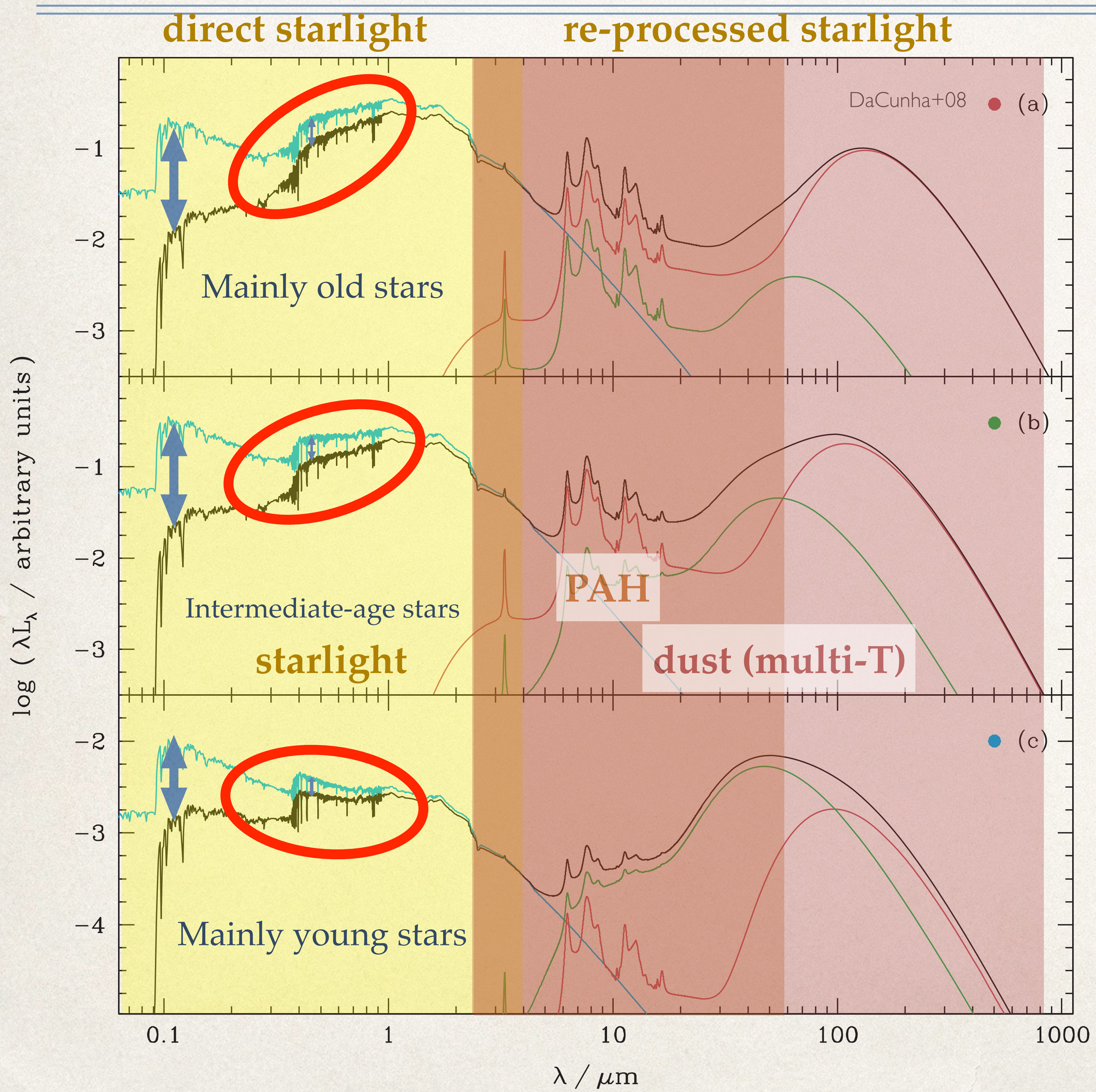

Note

- the different shape of the stellar continuum
  - emitted
  - attenuated (note dependence on λ)
- the corresponding shift of the dust emission
  - in Luminosity
  - in Temperature

Spectral Energy Distribution(s)

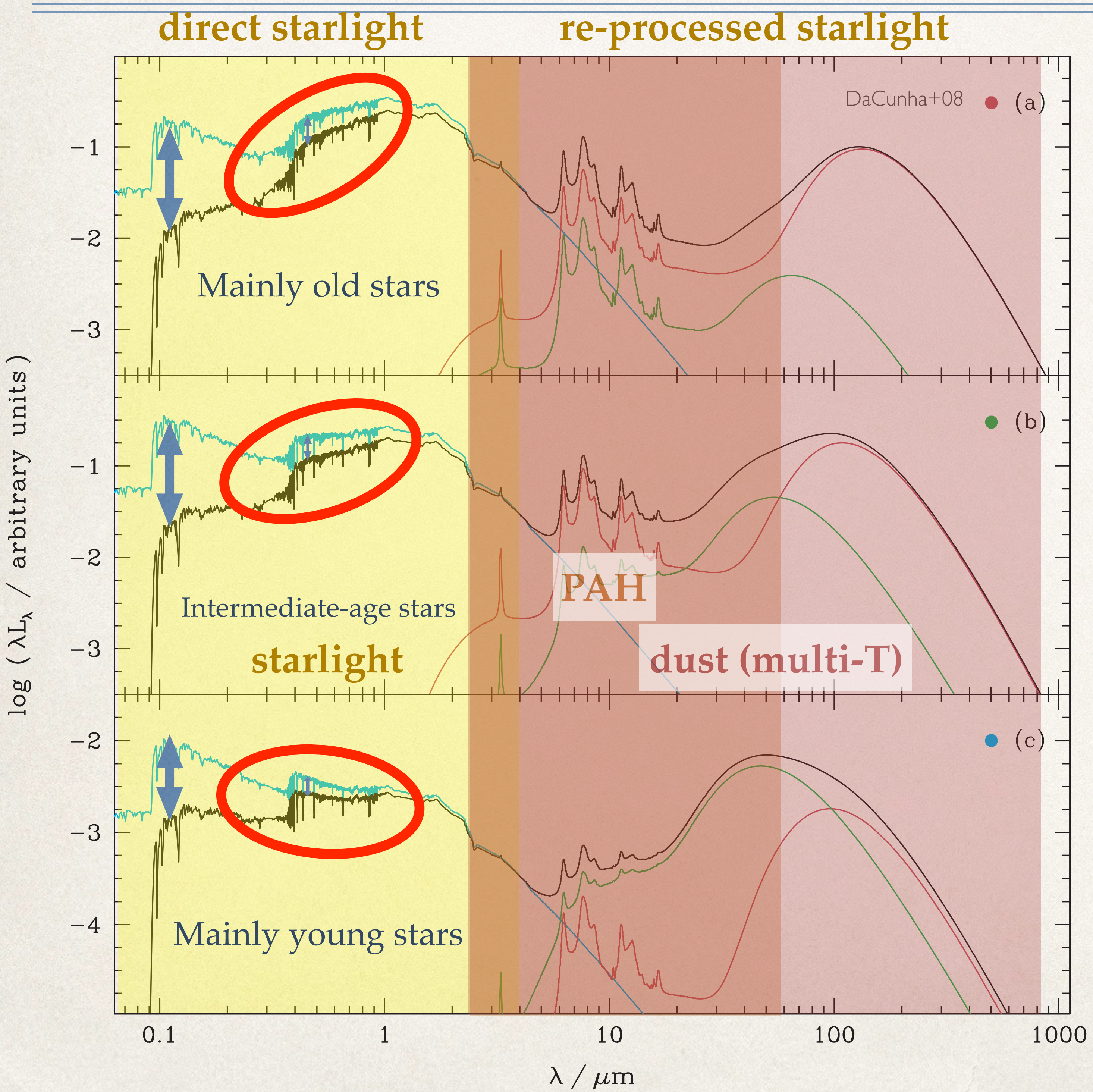

Note

- the different shape of the stellar continuum
  - emitted
  - attenuated (note dependence on λ)
- the corresponding shift of the dust emission
  - in Luminosity
  - in Temperature
  - in PAH relative contribution

Spectral Energy Distribution(s)

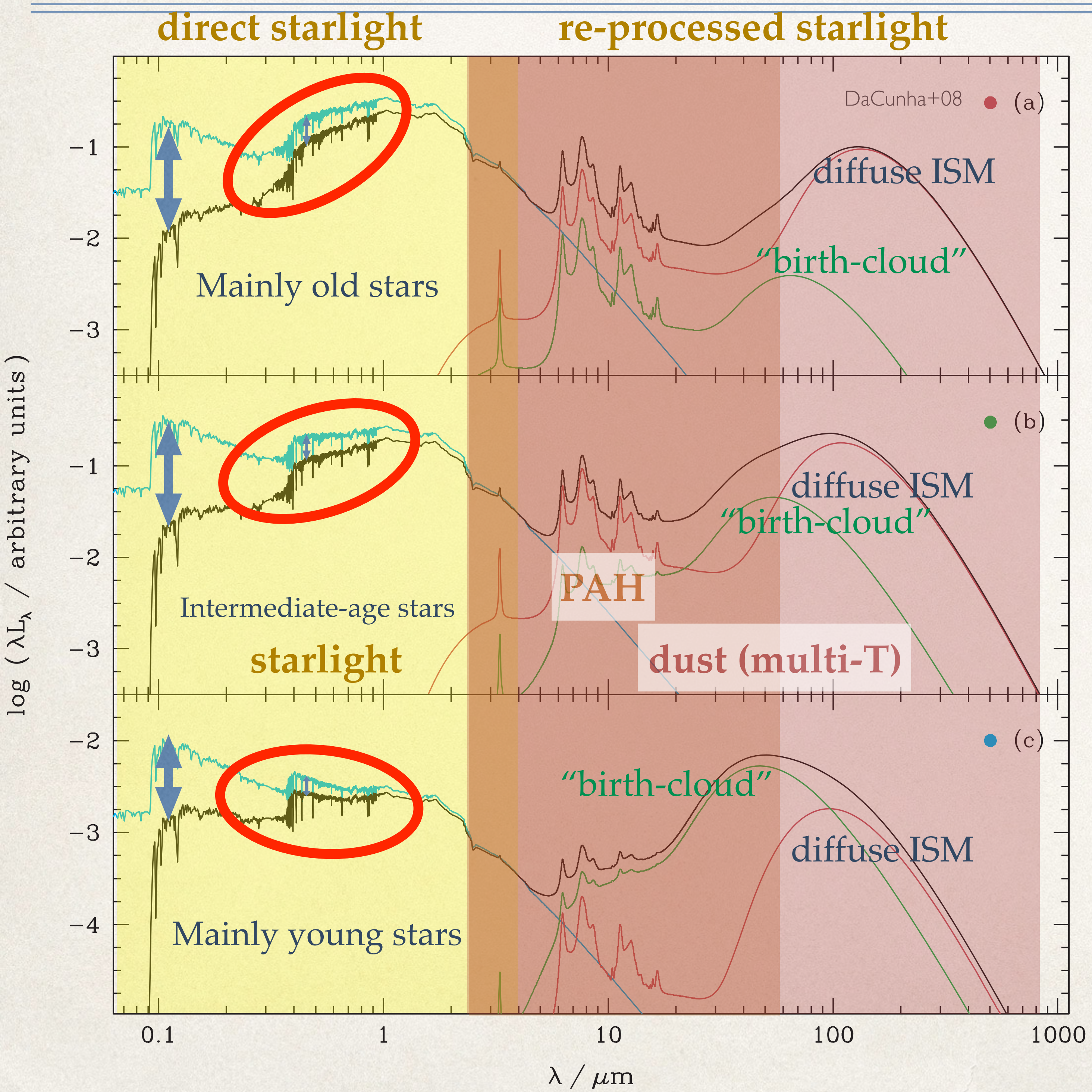

Note

- the different shape of the stellar continuum
  - emitted
  - attenuated (note dependence on λ)
- the corresponding shift of the dust emission
  - in Luminosity
  - in Temperature
  - in PAH relative contribution
- the change in relative contribution of diffuse ISM and "birth-cloud"

Spectral Energy Distributions

Models

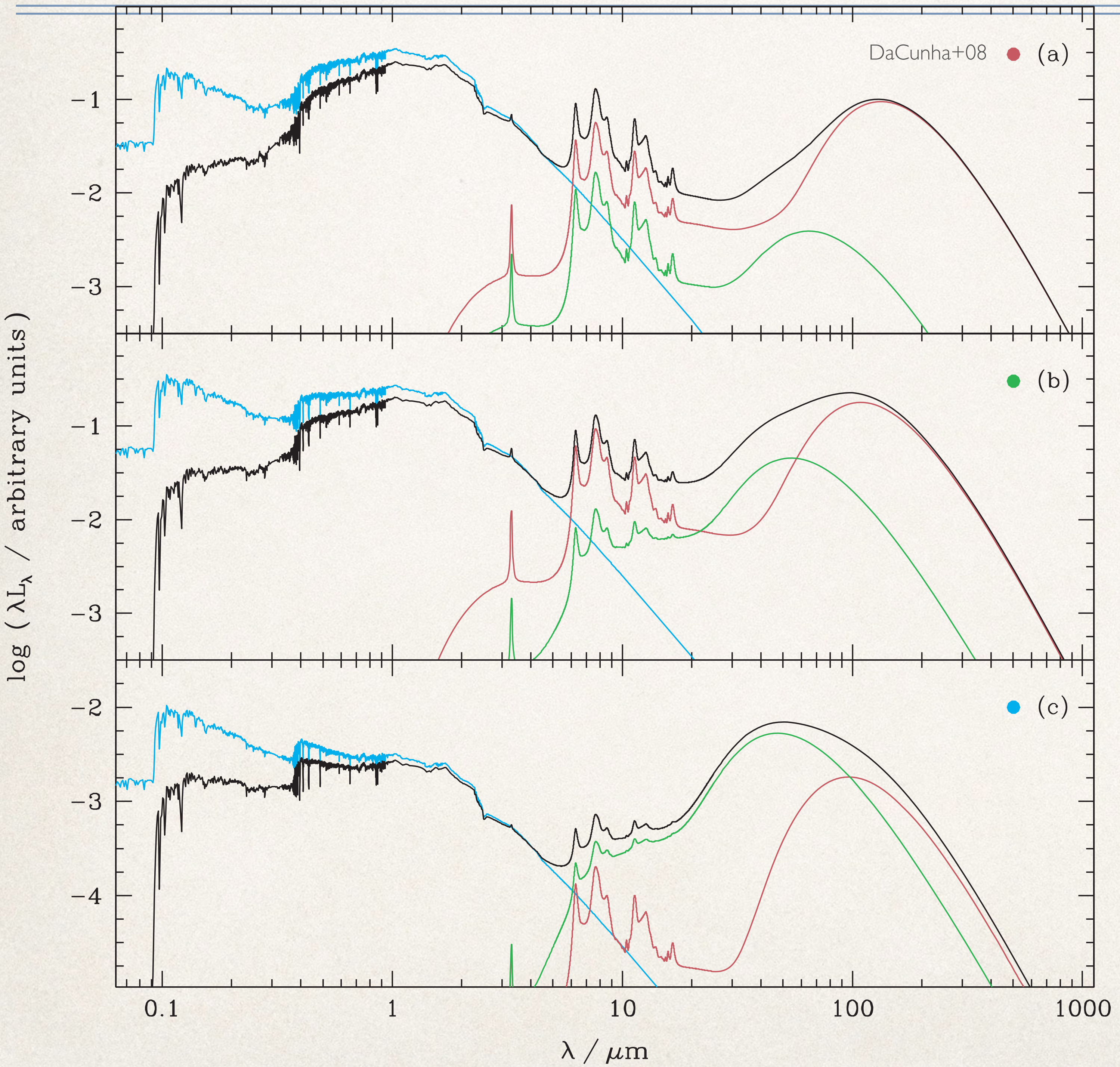

Spectral Energy Distributions

Models

Observations (templates)

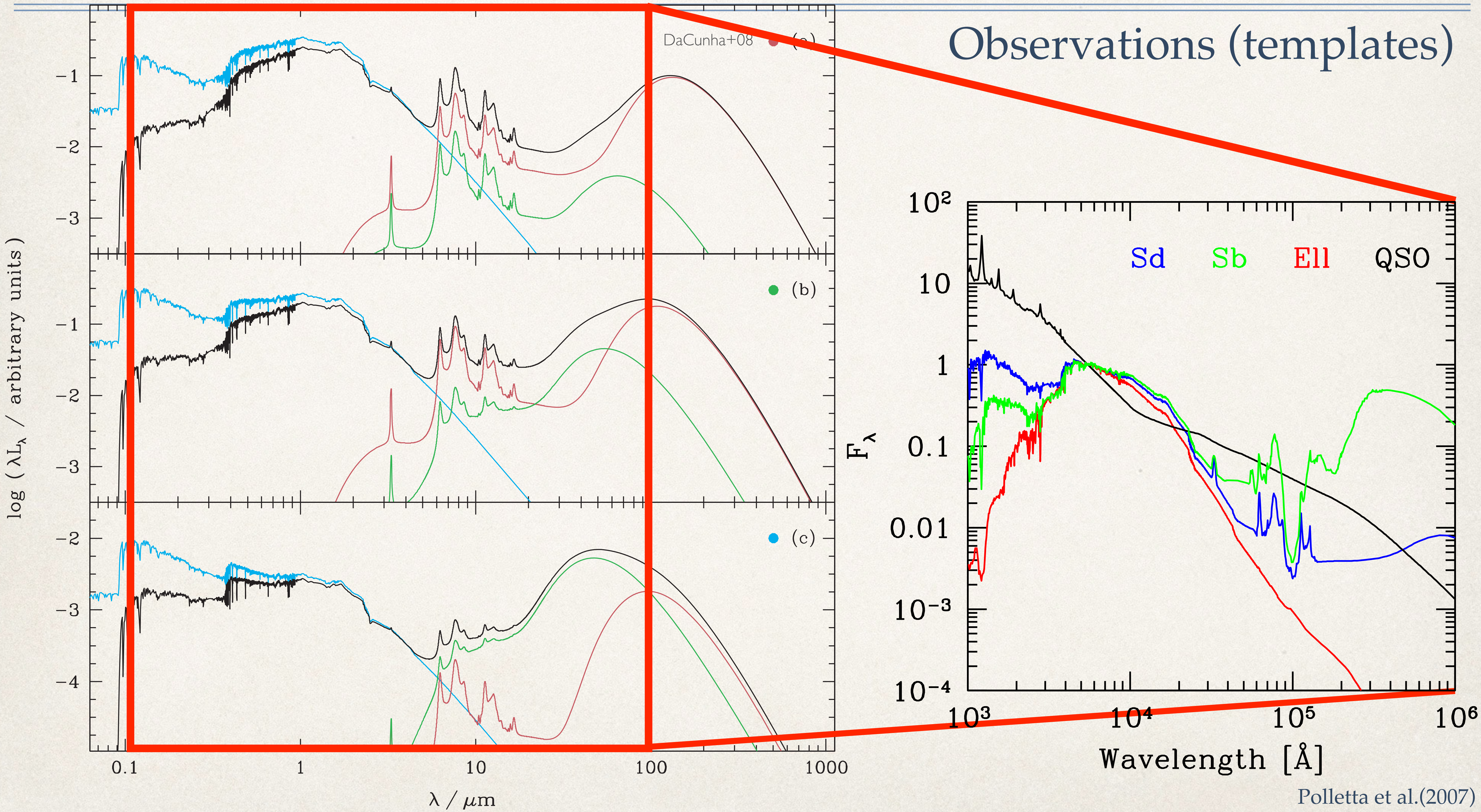

Polletta et al.(2007)

The Spectrum of Starlight

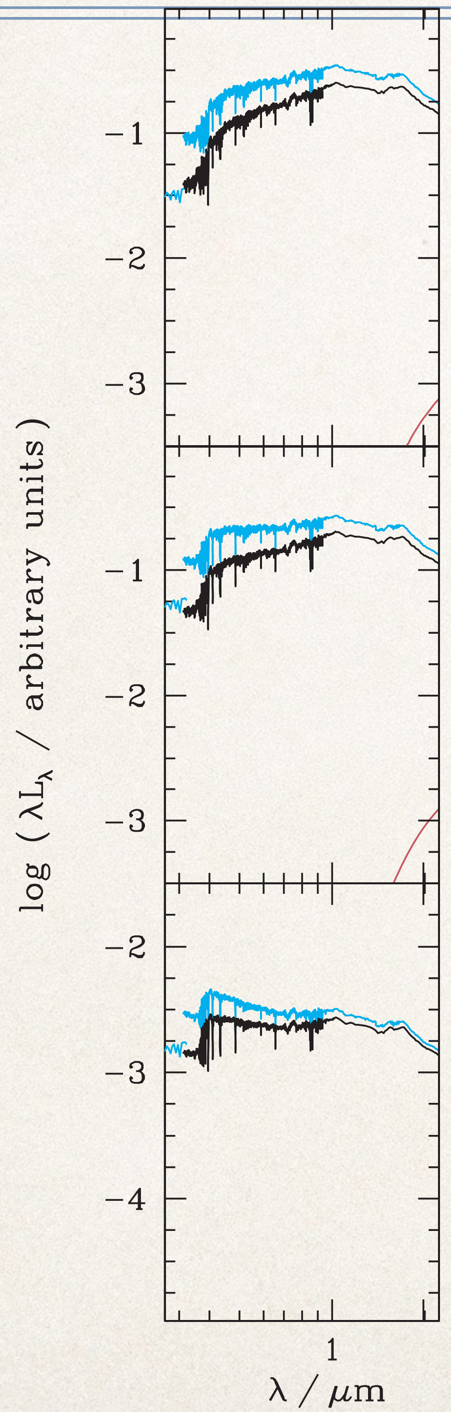

- (UV)-VIS-NIR: ~pure starlight
- Sum of spectra of all stars
- Attenuation by dust
  - absorption and re-radiation at different λ
  - effect of light scattered in and out the line of sight
  - not all stars suffer the same attenuation

Combining the spectra of stars

- Stellar spectra depend mainly on mass, age and chemical composition
- Need to know how many stars we have in this 3(+)D parameter space
  - initial conditions (Initial Mass Function)
  - time evolution of individual stellar spectra
  - time evolution of the mass function

The stellar zoo: the Hertzprung-Russell diagram

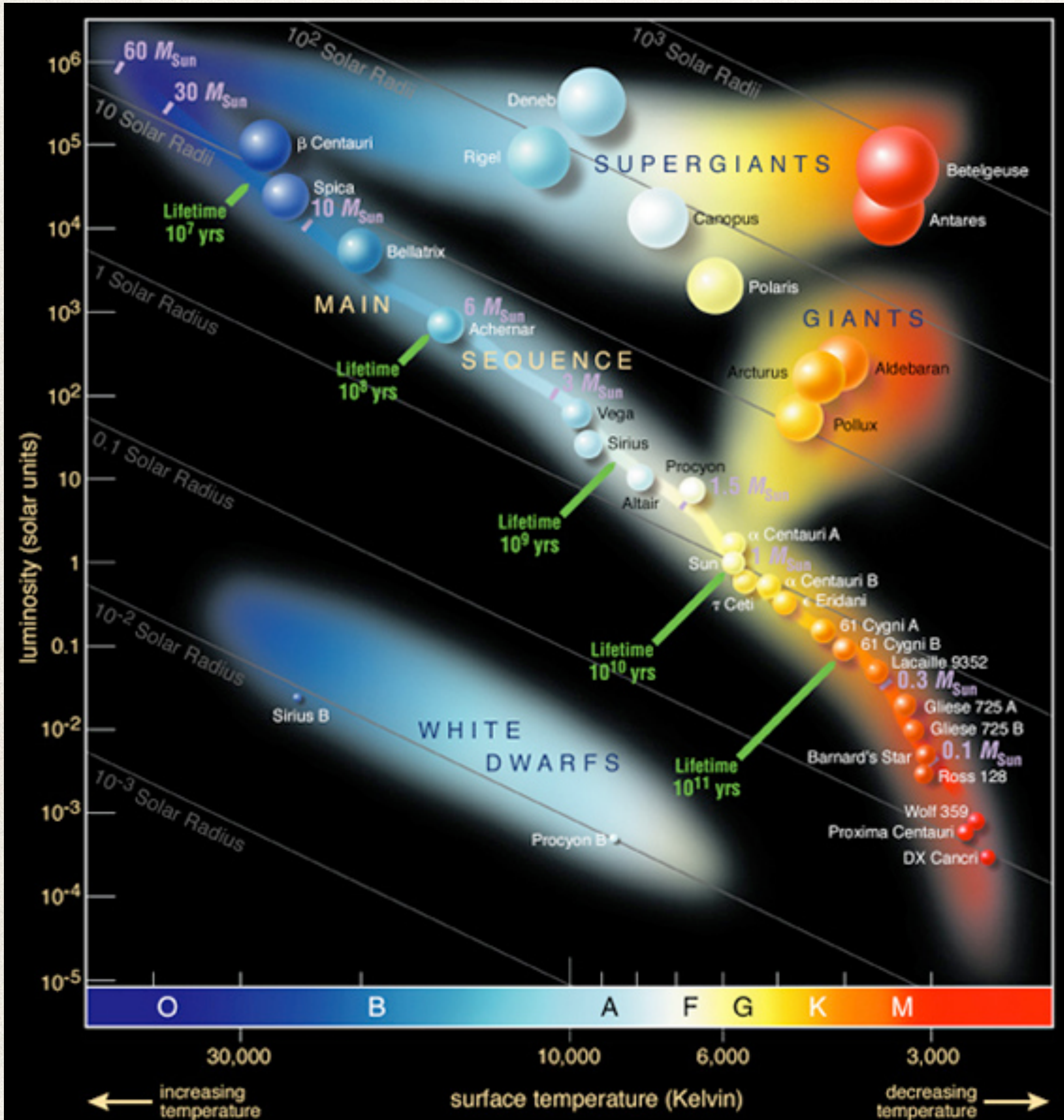

- Main Sequence — Hydrogen-core-burning stars

- Mass–luminosity relation ($0.1M_\odot < M < 100M_\odot$):

$$L \propto M^4 \quad \text{for} \quad M > 0.6M_\odot$$
$$L \propto M^2 \quad \text{for} \quad M < 0.6M_\odot$$

- Mass–radius relation:

$$R \propto M^{0.6} \quad \text{for} M > 0.6M_\odot$$

- Luminosity–temperature relation: $$L \propto T_{eff}^7$$

- Gravity

$$g \approx const \approx g_\odot$$

Stellar evolution to the Red Giant Branch (RGB)

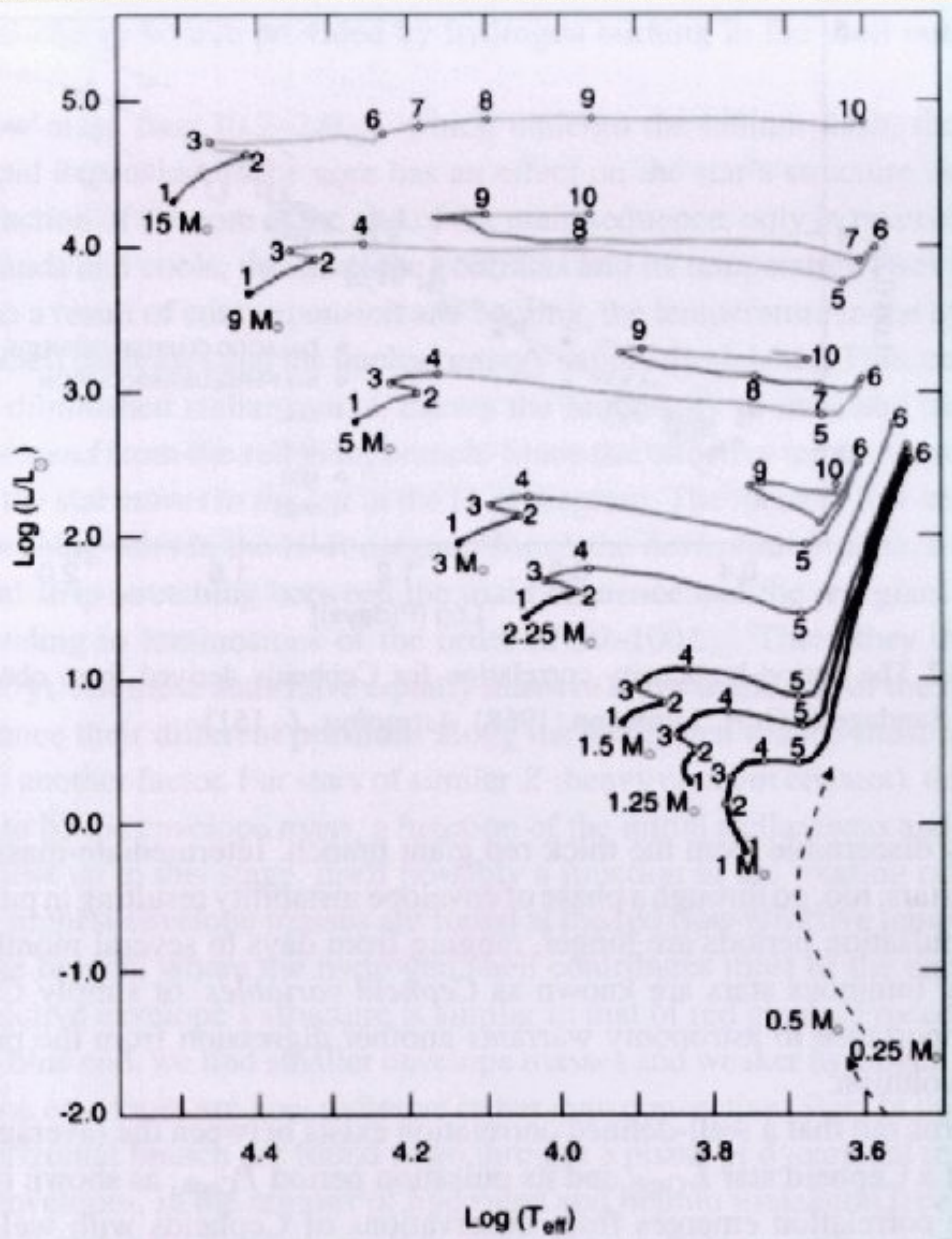

Evolutionary paths in the HRD up to the point where He burning sets in (from Iben 1967, ARAA 5). The shade of the line segments indicates the time spent in the corresponding phases.

MS (1-3) life-times:
1.0M$_\odot$: 9.0E9yrs
2.2M$_\odot$: 5.0E8yrs
15.M$_\odot$: 1E7yrs

GB (5-6) life-times:
1.0M$_\odot$: 1.0E9yrs
2.2M$_\odot$: 3.8E7yrs
15.M$_\odot$: 1.5E6yrs (6-10)

From IMPRS Astrophysics Introductory Course, Ralf Bender et al.

Stellar evolution after the RGB

Note: *As helium burning sets in at the same core mass, all mass poor stars have the same luminosity at the tip of the giant branch.*

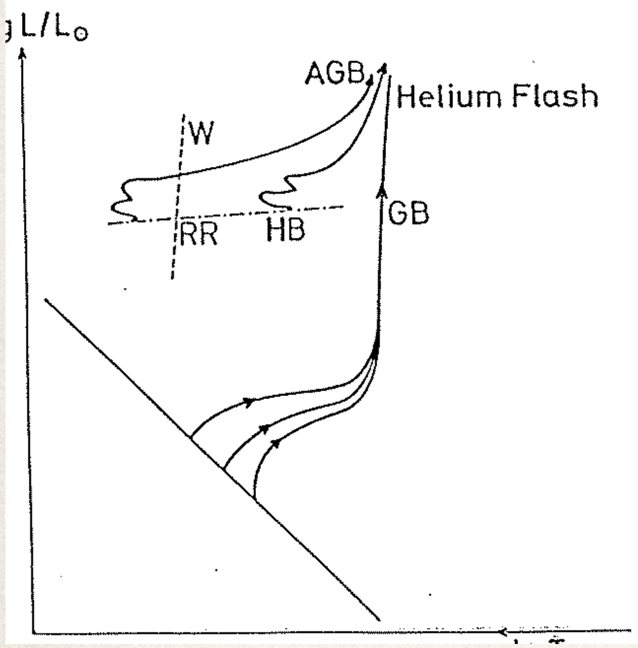

Fig. 32.10. Sketch of the evolution of low-mass stars in the HR diagram. For three slightly different masses the evolutionary tracks in the post-main-sequence merge in the giant branch (GB). After the helium flash they appear on the zero-age horizontal branch (HB), evolve towards the upper right, and merge in the asymptotic giant branch (AGB). The broken line indicates the positions of the variable RR Lyr stars (RR) and of the W Vir stars (W)

The post giant branch evolution is dependent on the mass:

- $M \lesssim 0.5 M_\odot$
  The pressure of the degenerated electron gas stops the contraction of the helium core before $T_c \approx 10^8$K is reached. $\Rightarrow$ no helium burning. H shell burning slowly stops, the star cools out.
- $0.5 M_\odot \lesssim M \lesssim 2.5 M_\odot$
  The H shell burning puts more and more He onto the core, which keeps contracting. Here too, the core is first degenerated but the temperature is rising until 10^8K is finally reached and He–burning starts. Because pressure equilibrium was maintained by the degeneracy of the electron gas, T_c is rising while P_c doesn't (Pauli principle). Therefore no expansion can moderate the reactor and T_c rises. Because $\epsilon_{3\alpha} \propto T_c^{30}$ the energy production increases dramatically.

  $\Rightarrow$ thermonuclear runaway!

  This stops once T_c is high enough to remove the degeneracy, i.e. at $(T_c > T_{\text{Fermi}})$. The star expands on a hydrostatic time scale and reaches its highest luminosity at the tip of the giant branch:$\Rightarrow$ Helium flash

From IMPRS Astrophysics Introductory Course, Ralf Bender et al.

- Massive stars with $M > 2.5 M_\odot$

  Mostly the same evolution as for less massive stars. But, before ignition of helium burning the electron gas is not degenerated, thus we have a continous transition to helium burning. The star performs loops in the HRD at nearly constant luminosity.

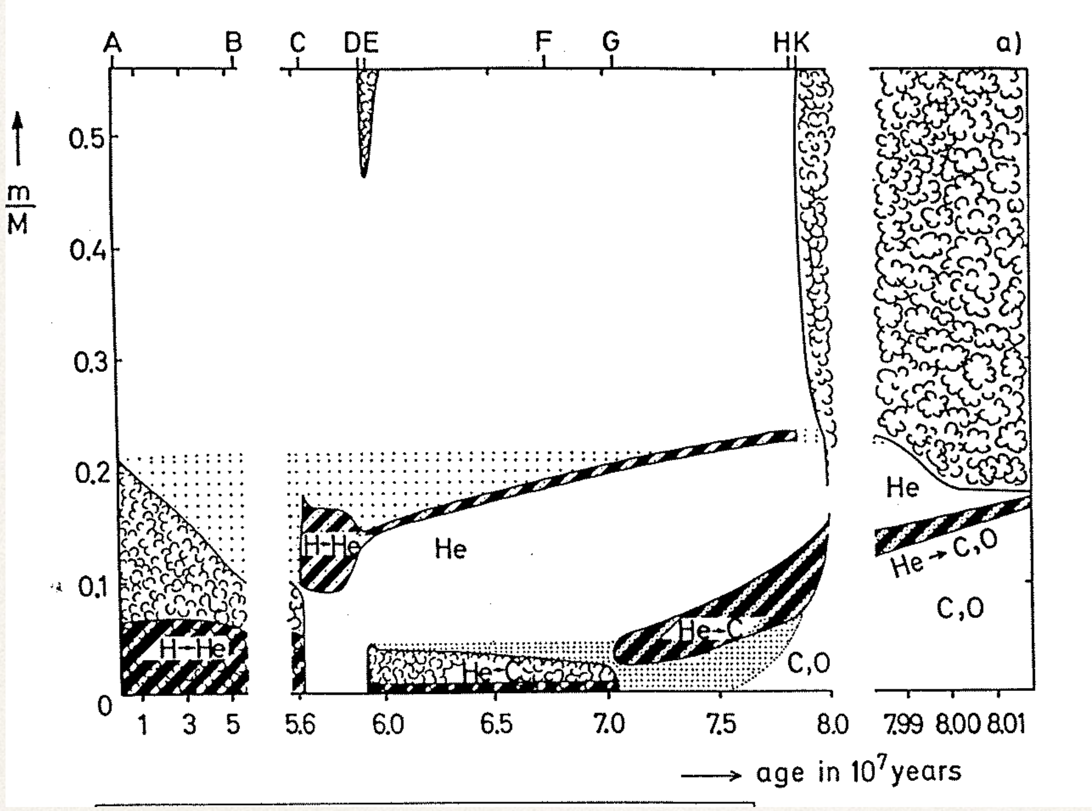

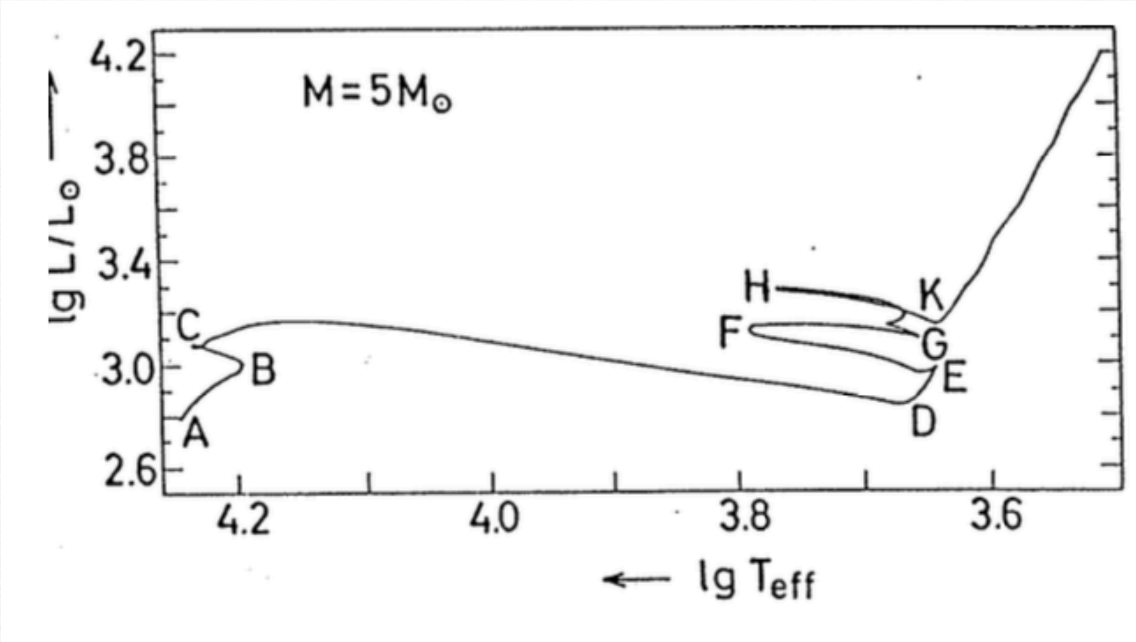

Evolution of a 5 solar mass star (Kippenhahn/Weigert).

Stellar evolution at different masses

Star in a box!

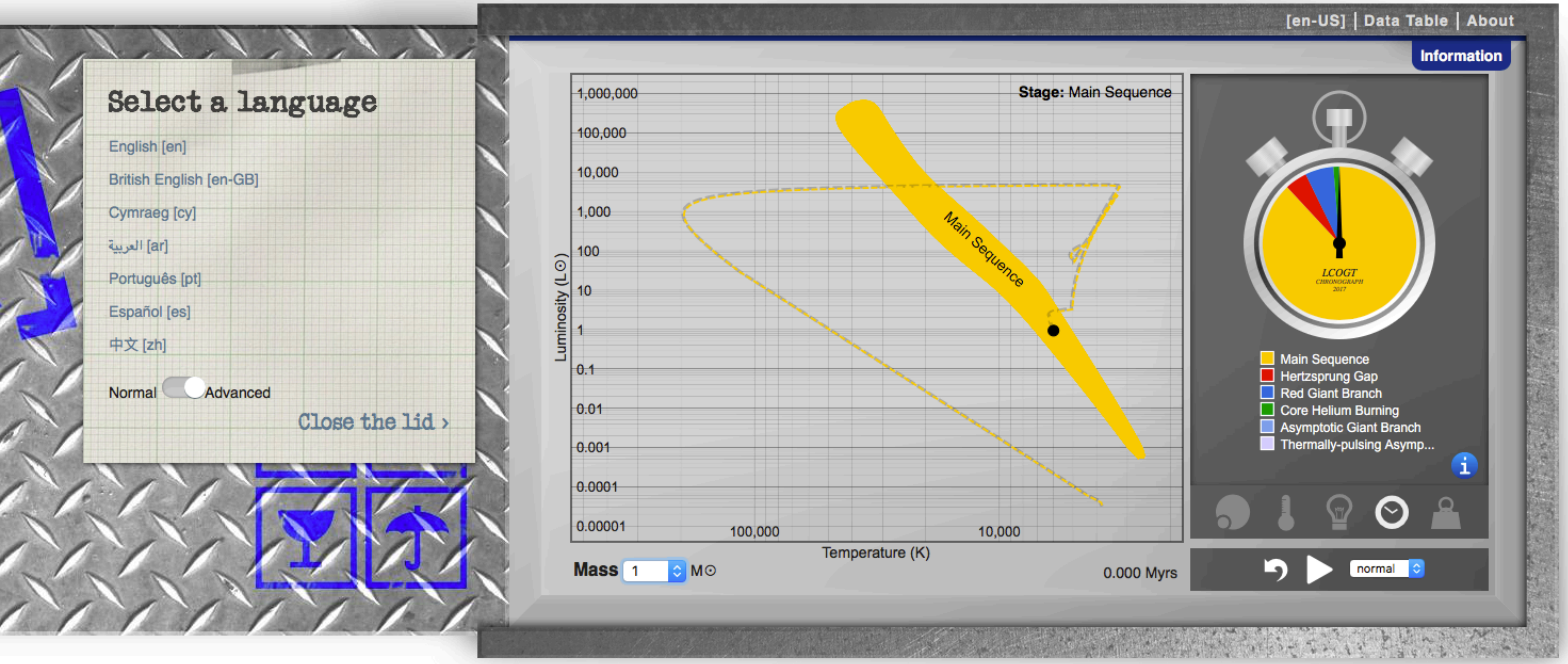

Simple Stellar Populations (SSP)
Initial Mass Function

- Simple Stellar Population (SSP): a set of coeval stars drawn from an initial distribution in mass (Initial Mass Function or IMF)
- IMF is thought to be universal or "semi-universal" (with some parametric dependence on "external condition"). This has to do with the physics of star formation

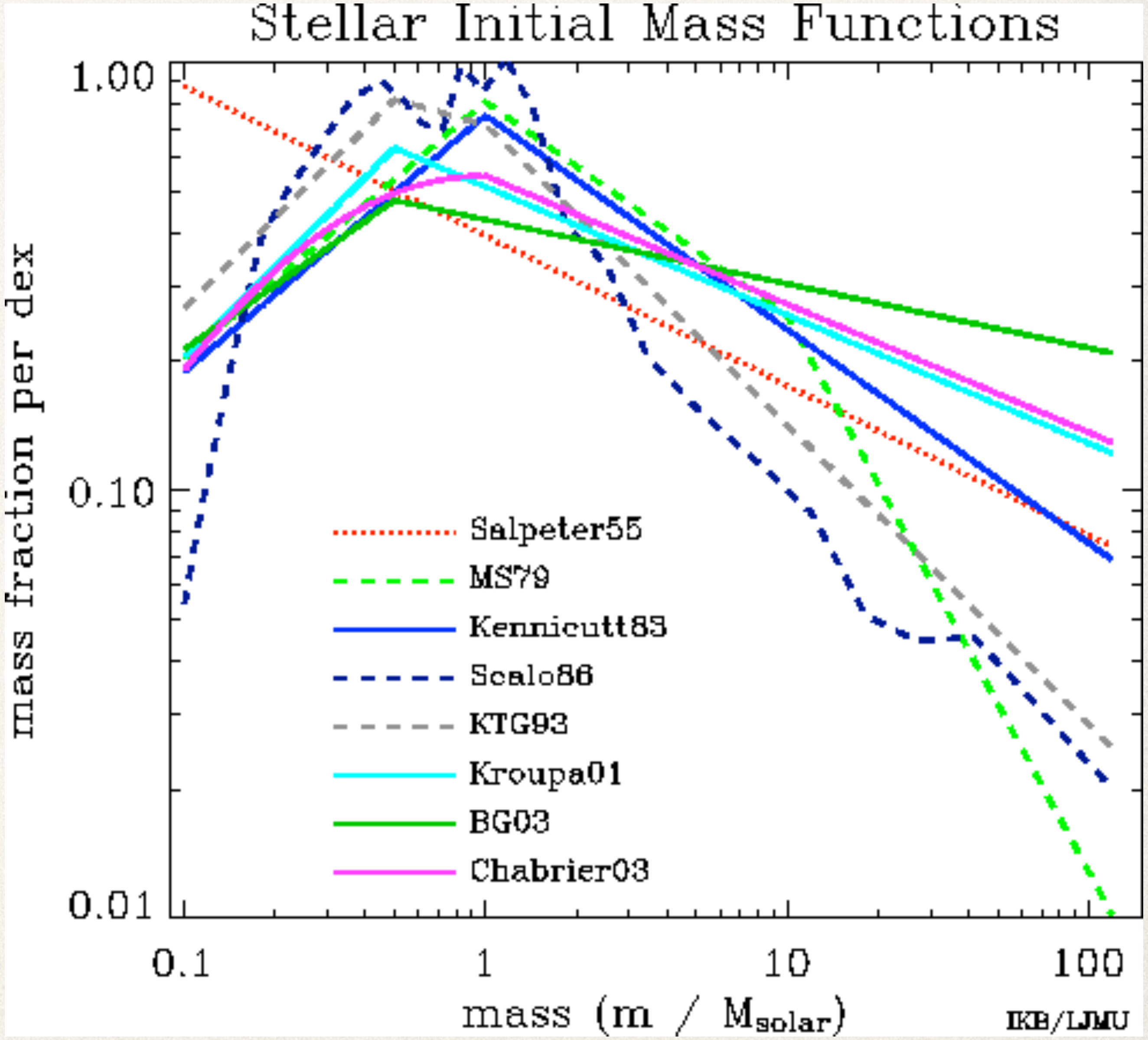

from Ivan Baldry's webpage

http://www.astro.ljmu.ac.uk/~ikb/research/imf-use-in-cosmology.html

Simple Stellar Populations (SSP) Evolutionary Tracks, Isochrones, CMDs

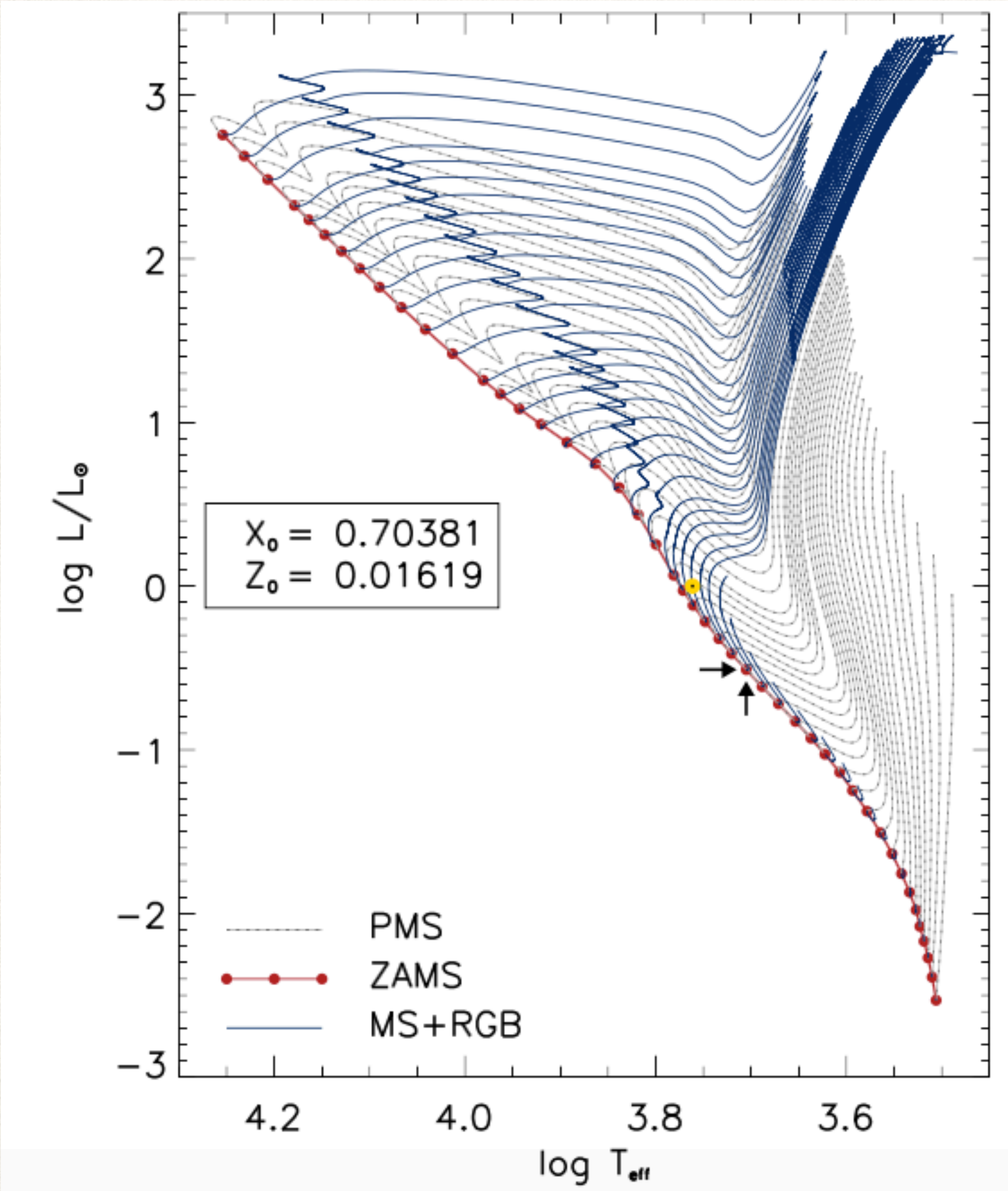

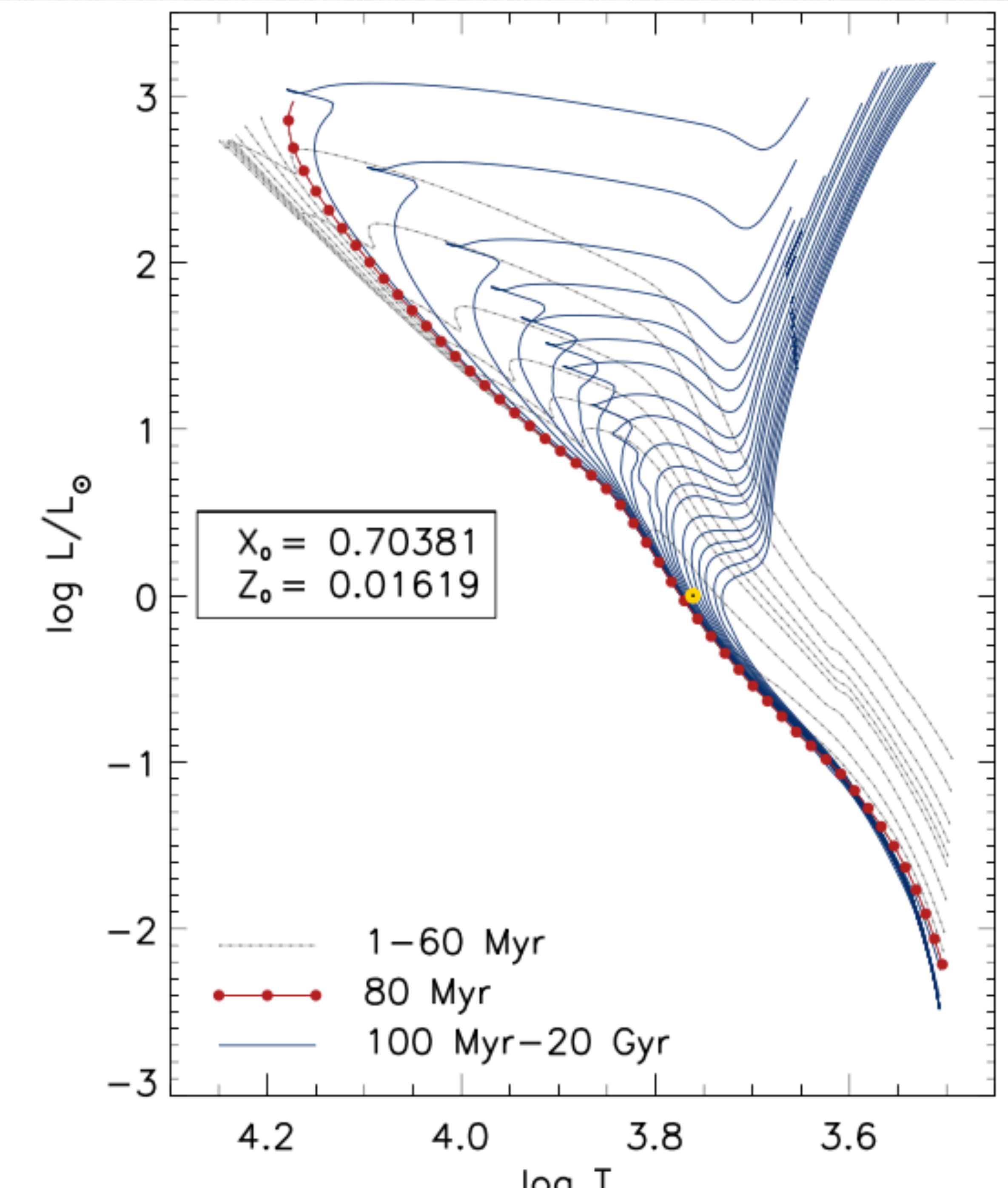

Spada et al. (2017)

Stellar Spectra

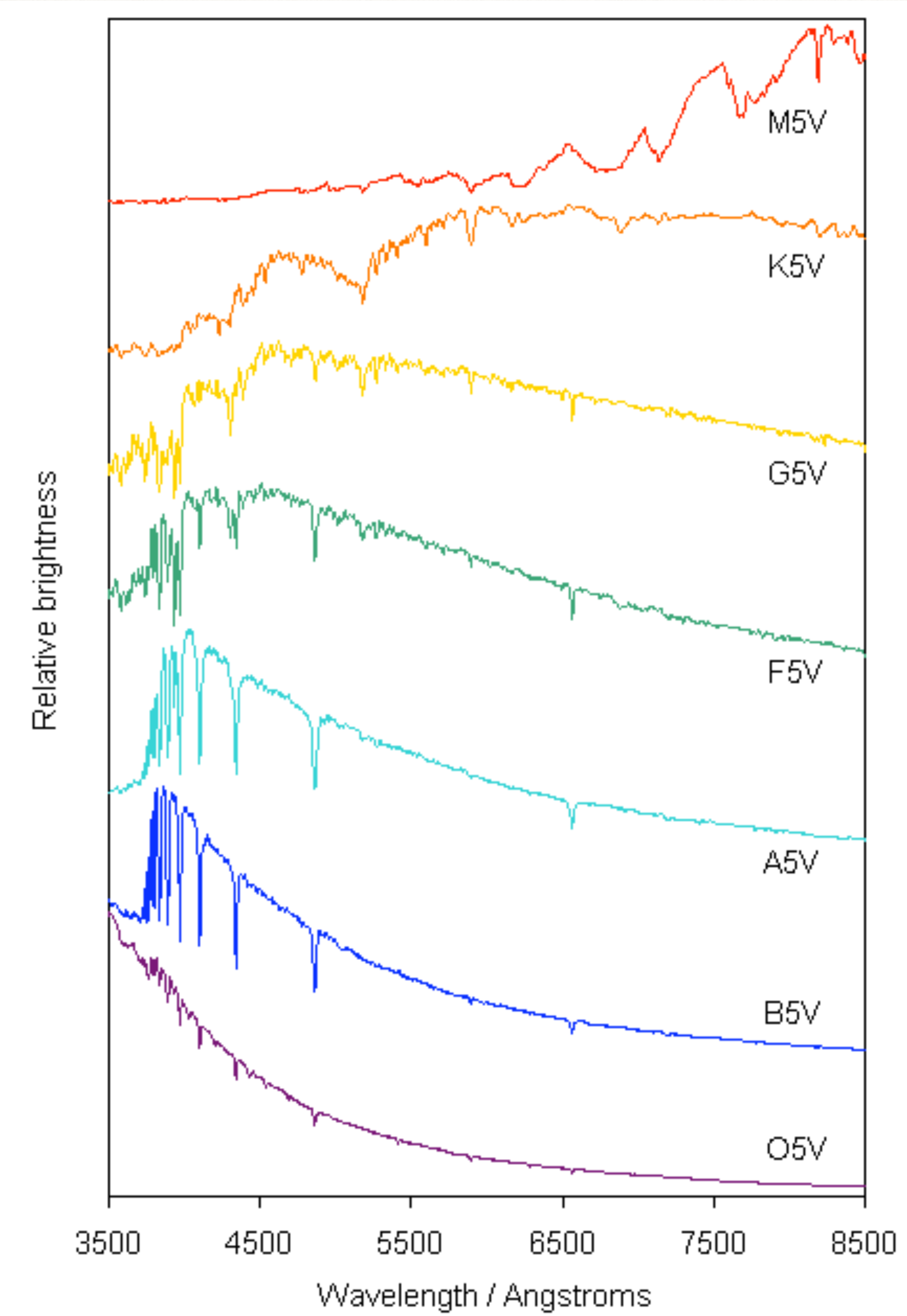

Type	Colour	Approximate Surface Temperature	Main Characteristics	Examples
O	Blue	> 25,000 K	Singly ionized helium lines either in emission or absorption. Strong ultraviolet continuum.	10 Lacertra
B	Blue	11,000 - 25,000	Neutral helium lines in absorption.	Rigel Spica
A	Blue	7,500 - 11,000	Hydrogen lines at maximum strength for A0 stars, decreasing thereafter.	Sirius Vega
F	Blue to White	6,000 - 7,500	Metallic lines become noticeable.	Canopus, Procyon
G	White to Yellow	5,000 - 6,000	Solar-type spectra. Absorption lines of neutral metallic atoms and ions (e.g. once-ionized calcium) grow in strength.	Sun, Capella
K	Orange to Red	3,500 - 5,000	Metallic lines dominate. Weak blue continuum.	Arcturus, Aldebaran
M	Red	< 3,500	Molecular bands of titanium oxide noticeable.	Betelgeuse, Antares

Stellar Spectra: main absorption features

- Hydrogen Balmer lines
- Balmer break

Transition of *n*	3→2	4→2	5→2	6→2	7→2	8→2	9→2	∞→2
Name	H-α / Ba-α	H-β / Ba-β	H-γ / Ba-γ	H-δ / Ba-δ	H-ε / Ba-ε	H-ζ / Ba-ζ	H-η / Ba-η	Balmer break
Wavelength (nm)[2]	656.3	486.1	434.1	410.2	397.0	388.9	383.5	364.6
Energy difference (eV)	1.89	2.55	2.86	3.03	3.13	3.19	3.23	3.40
Color	Red	Aqua	Blue	Violet	(Ultraviolet)	(Ultraviolet)	(Ultraviolet)	(Ultraviolet)

- D4000 break (not the same as Balmer break)

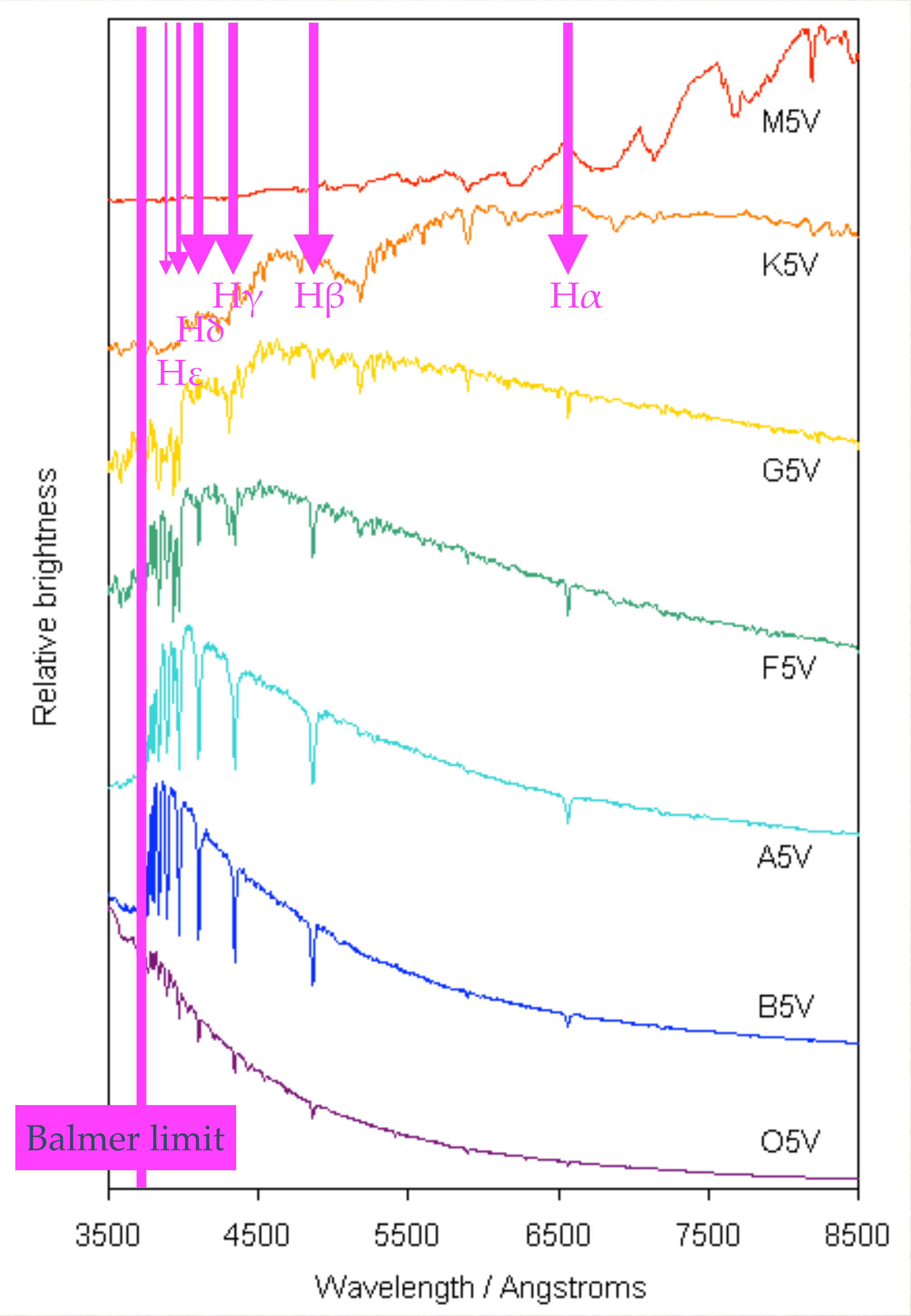

Stellar Spectra: main absorption features

- "Metal" absorption lines/complexes

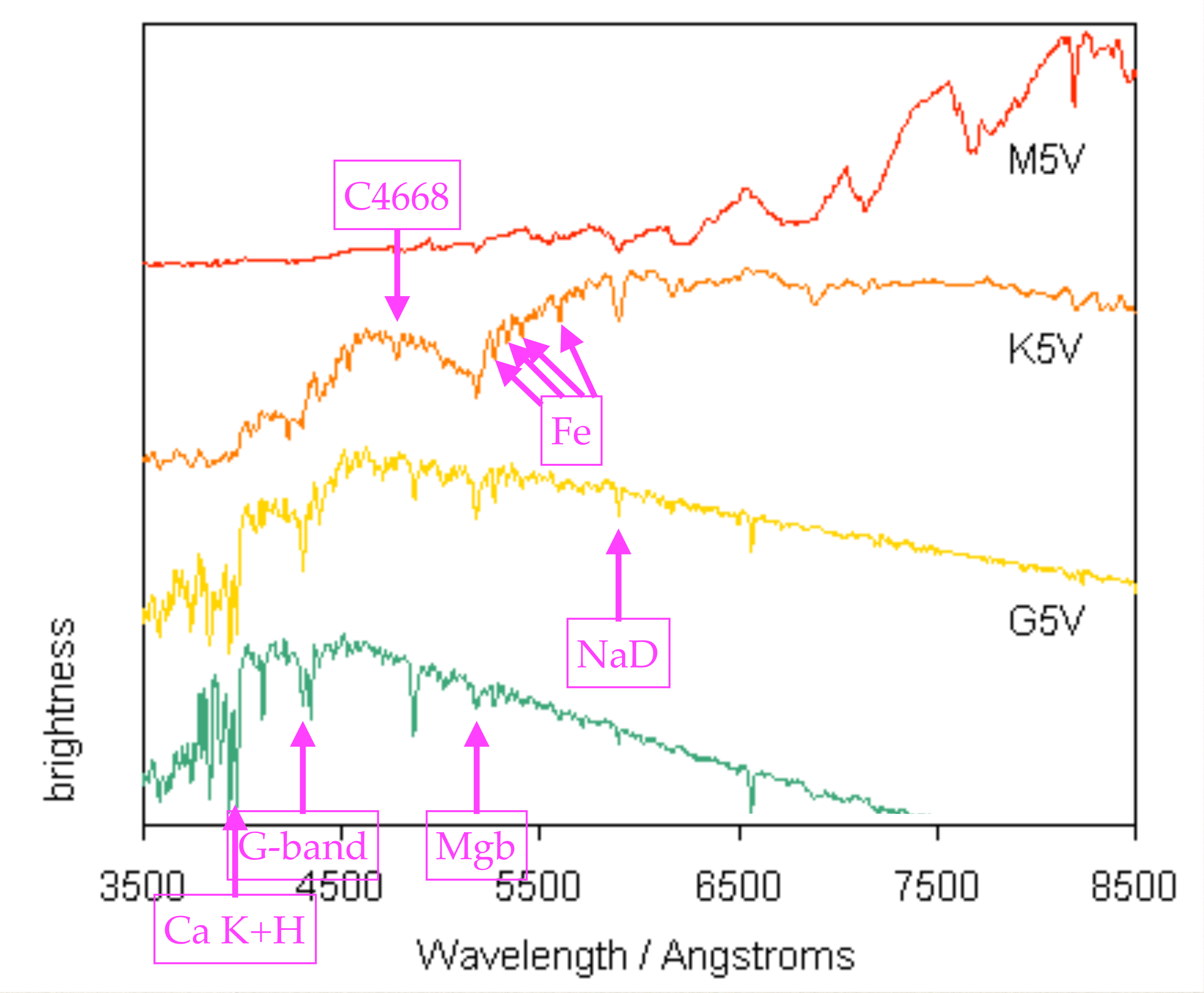

Galaxy Stellar Spectra: main absorption features

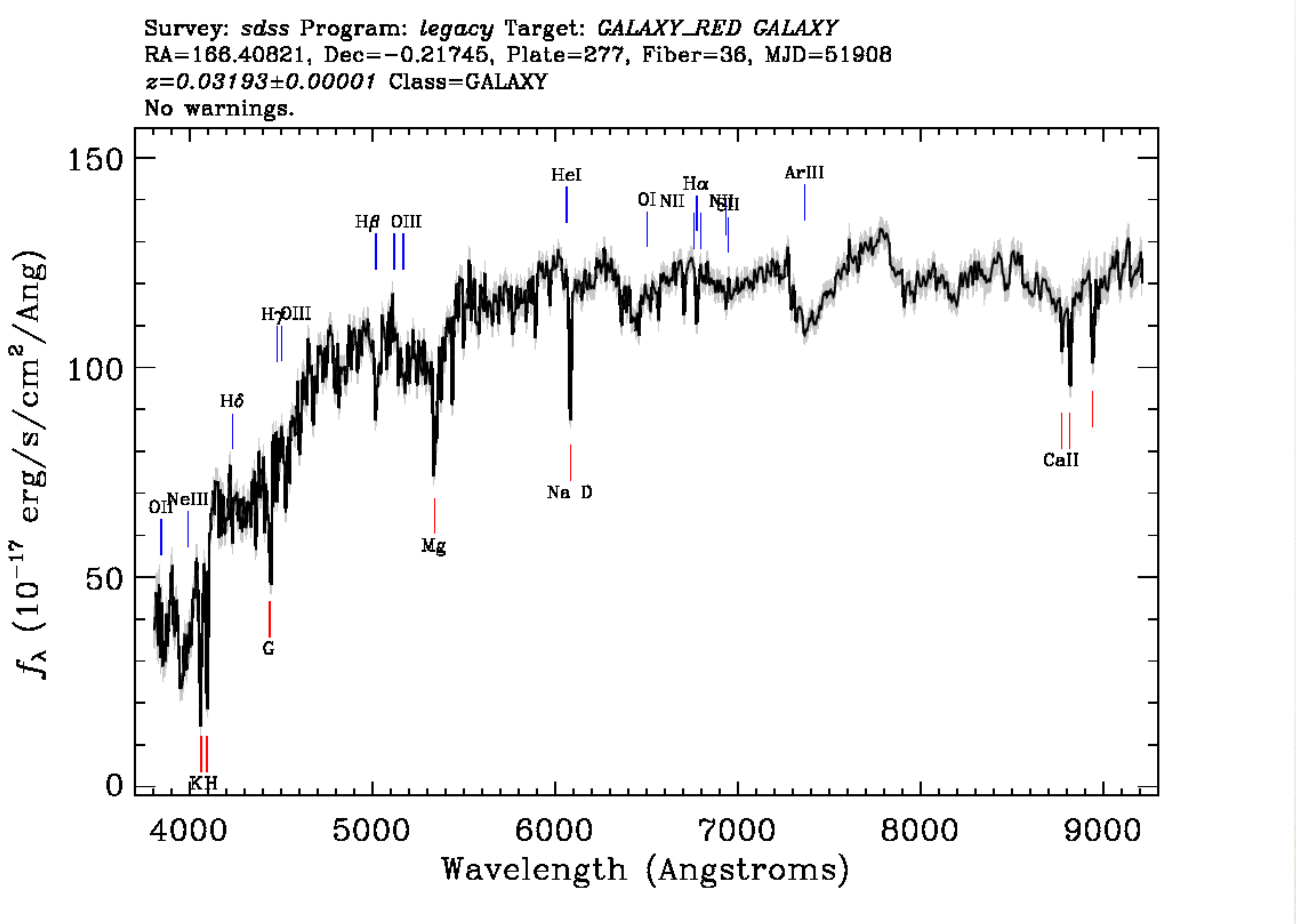

Measures of absorption lines/features

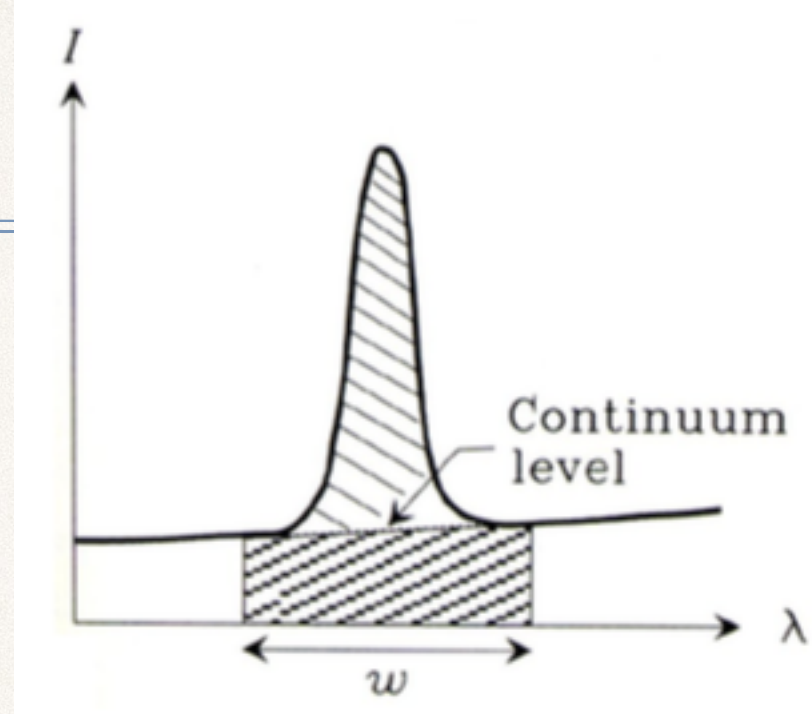

$$w = \int_{line} R_\lambda d\lambda = \int_{line} \frac{I_{\rm cont} - I_\lambda}{I_{\rm cont}} d\lambda$$

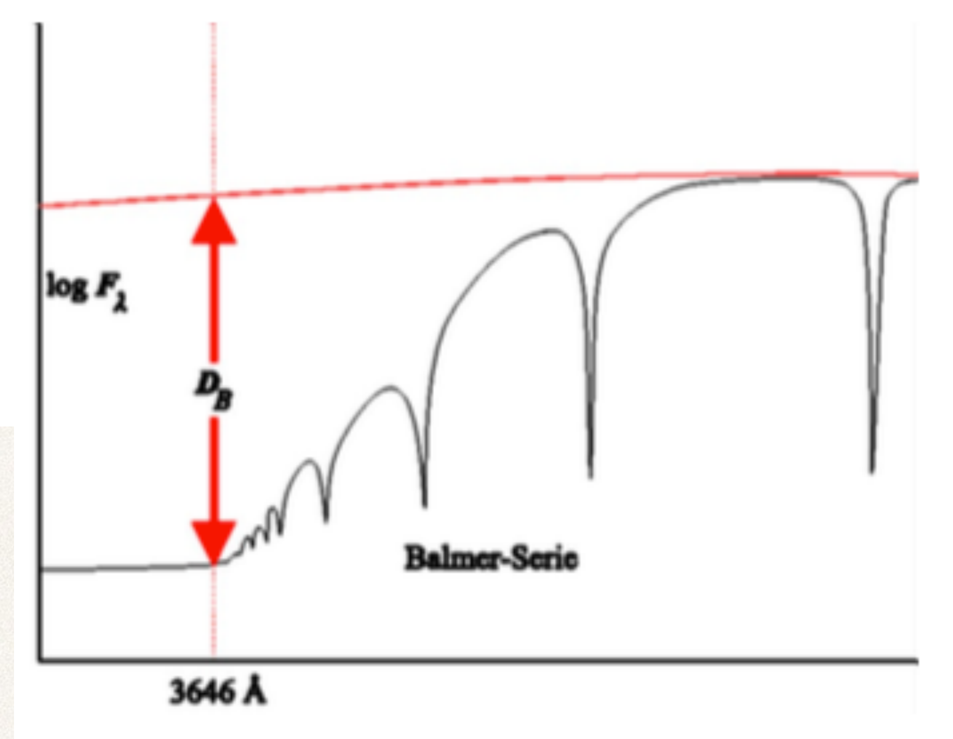

- Equivalent width
- Break:
  specific flux ratio
  red-ward and
  blue-ward of a spectral "jump"
- "Indices"
  - In real stellar/galaxy spectra there is no such thing as "continuum", but only a "pseudo-continuum" with a large number of absorption lines (blended at typical resolution for galaxy spectra)
  - Continuum level and line flux defined in side-bands and central band

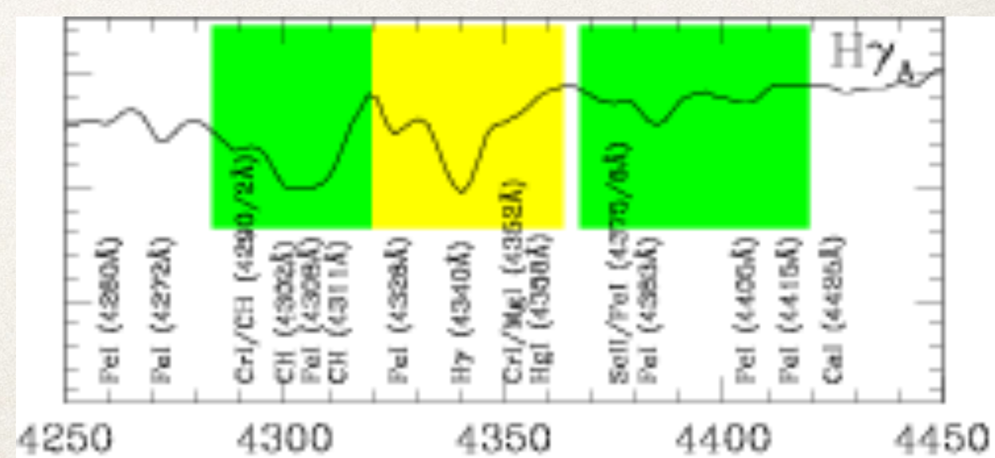

Puzia et al. (2013)

Examples of absorption indices

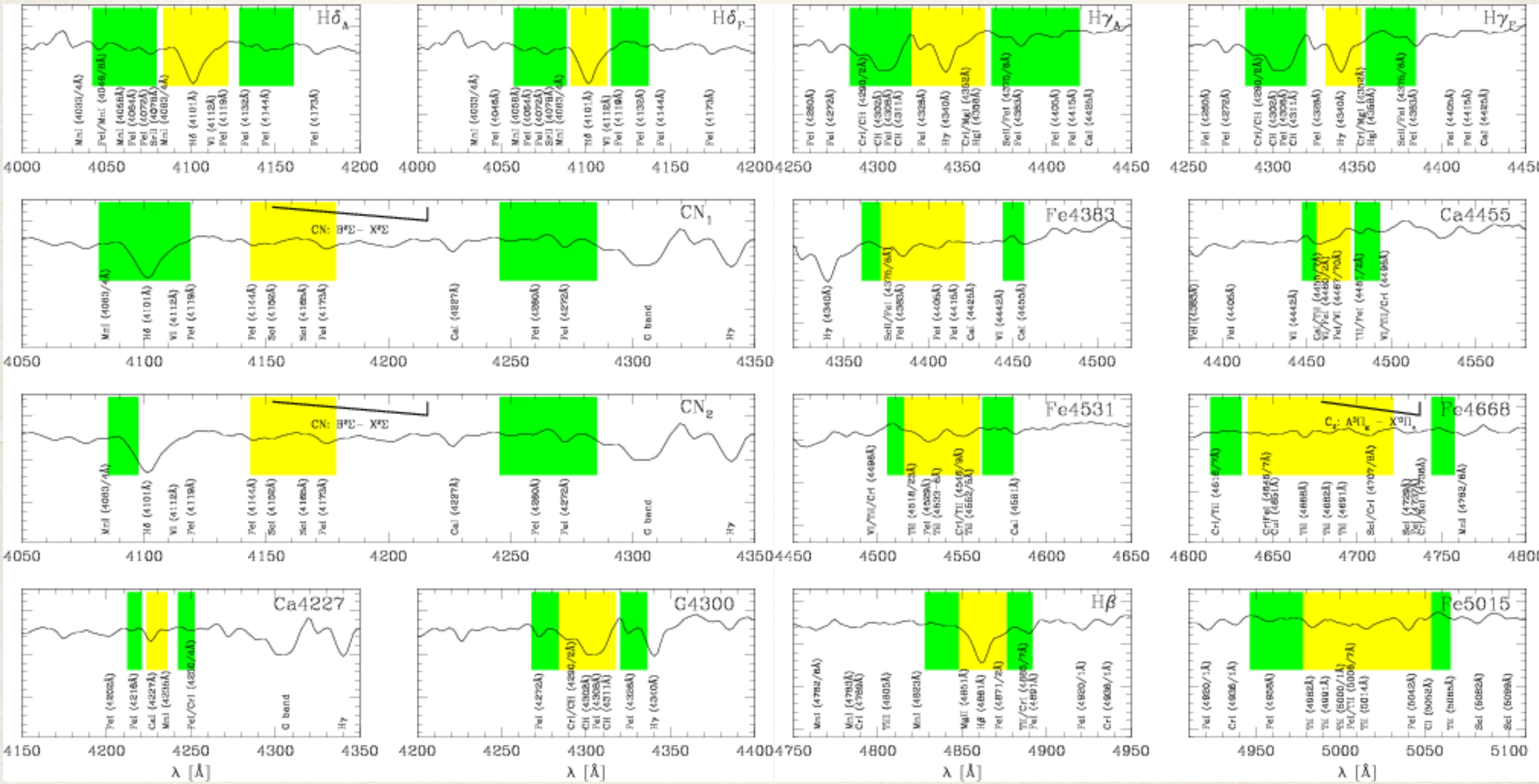

Puzia et al. (2013)

Examples of absorption indices

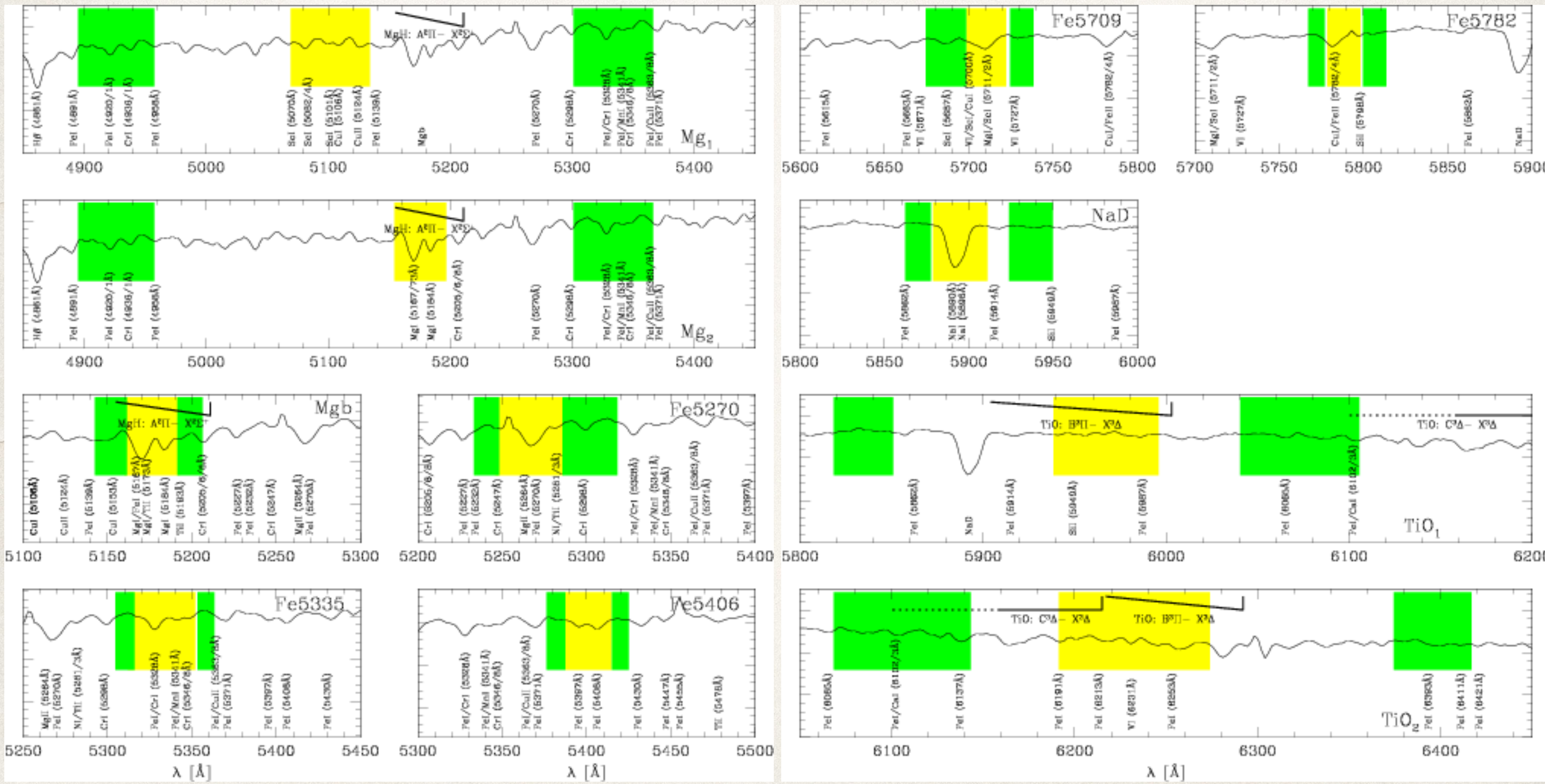

Puzia et al. (2013)

A list of "popular" indices

```
################################################################################
# Index Name    Index wl range        Blue cont wl range  Red cont wl range  Units
################################################################################

     Lick_CN1 4142.125 4177.125 4080.125 4117.625 4244.125 4284.125  mag
     Lick_CN2 4142.125 4177.125 4083.875 4096.375 4244.125 4284.125  mag
  Lick_Ca4227 4222.250 4234.750 4211.000 4219.750 4241.000 4251.000  A
   Lick_G4300 4281.375 4316.375 4266.375 4282.625 4318.875 4335.125  A
  Lick_Fe4383 4369.125 4420.375 4359.125 4370.375 4442.875 4455.375  A
  Lick_Ca4455 4452.125 4474.625 4445.875 4454.625 4477.125 4492.125  A
  Lick_Fe4531 4514.250 4559.250 4504.250 4514.250 4560.500 4579.250  A
   Lick_C4668 4634.000 4720.250 4611.500 4630.250 4742.750 4756.500  A
   Lick_Hb    4847.875 4876.625 4827.875 4847.875 4876.625 4891.625  A
  Lick_Fe5015 4977.750 5054.000 4946.500 4977.750 5054.000 5065.250  A
     Lick_Mg1 5069.125 5134.125 4895.125 4957.625 5301.125 5366.125  mag
     Lick_Mg2 5154.125 5196.625 4895.125 4957.625 5301.125 5366.125  mag
     Lick_Mgb 5160.125 5192.625 5142.625 5161.375 5191.375 5206.375  A
  Lick_Fe5270 5245.650 5285.650 5233.150 5248.150 5285.650 5318.150  A
  Lick_Fe5335 5312.125 5352.125 5304.625 5315.875 5353.375 5363.375  A
  Lick_Fe5406 5387.500 5415.000 5376.250 5387.500 5415.000 5425.000  A
  Lick_Fe5709 5696.625 5720.375 5672.875 5696.625 5722.875 5736.625  A
  Lick_Fe5782 5776.625 5796.625 5765.375 5775.375 5797.875 5811.625  A
     Lick_NaD 5876.875 5909.375 5860.625 5875.625 5922.125 5948.125  A
    Lick_TiO1 5936.625 5994.125 5816.625 5849.125 6038.625 6103.625  mag
    Lick_TiO2 6189.625 6272.125 6066.625 6141.625 6372.625 6415.125  mag
Lick_Hd_A     4083.500 4122.250 4041.600 4079.750 4128.500 4161.000 A
Lick_Hg_A     4319.750 4363.500 4283.500 4319.750 4367.250 4419.750 A
Lick_Hd_F     4091.000 4112.250 4057.250 4088.500 4114.750 4137.250 A
Lick_Hg_F     4331.250 4352.250 4283.500 4319.750 4354.750 4384.750 A
DTT_CaII8498  8483.000 8513.000 8447.500 8462.500 8842.500 8857.500  A
DTT_CaII8542  8527.000 8557.000 8447.500 8462.500 8842.500 8857.500  A
DTT_CaII8662  8647.000 8677.000 8447.500 8462.500 8842.500 8857.500  A
DTT_MgI8807   8799.500 8814.500 8775.000 8787.000 8845.000 8855.000  A
 BH_CNB        3810.0    3910.0    3785.0    3810.0    3910.0    3925.0    mag
 BH_HK         3925.0    3995.0    3910.0    3925.0    3995.0    4010.0    mag
 BH_CaI        4215.0    4245.0    4200.0    4215.0    4245.0    4260.0    mag
 BH_G          4285.0    4315.0    4275.0    4285.0    4315.0    4325.0    mag
 BH_Hb         4830.0    4890.0    4800.0    4830.0    4890.0    4920.0    mag
 BH_MgG        5150.0    5195.0    5125.0    5150.0    5195.0    5220.0    mag
 BH_MH         4940.0    5350.0    4740.0    4940.0    5350.0    5550.0    mag
 BH_FC         5250.0    5280.0    5225.0    5250.0    5280.0    5305.0    mag
 BH_NaD        5865.0    5920.0    5835.0    5865.0    5920.0    5950.0    mag

################################################################################
# Lick indices from Worthey et al., 1994, ApJS, 94, 687 &
# Worthey and Ottaviani, 1997, ApJS, 111, 377
# BH indices from Brodie and Hanes (see Huchra et al. 1996, ApJS, 102, 29)
# DTT indices from Diaz, Terlevich, & Terlevich, 1989, MNRAS, 239, 325
################################################################################
```

Time evolution of SSP spectra

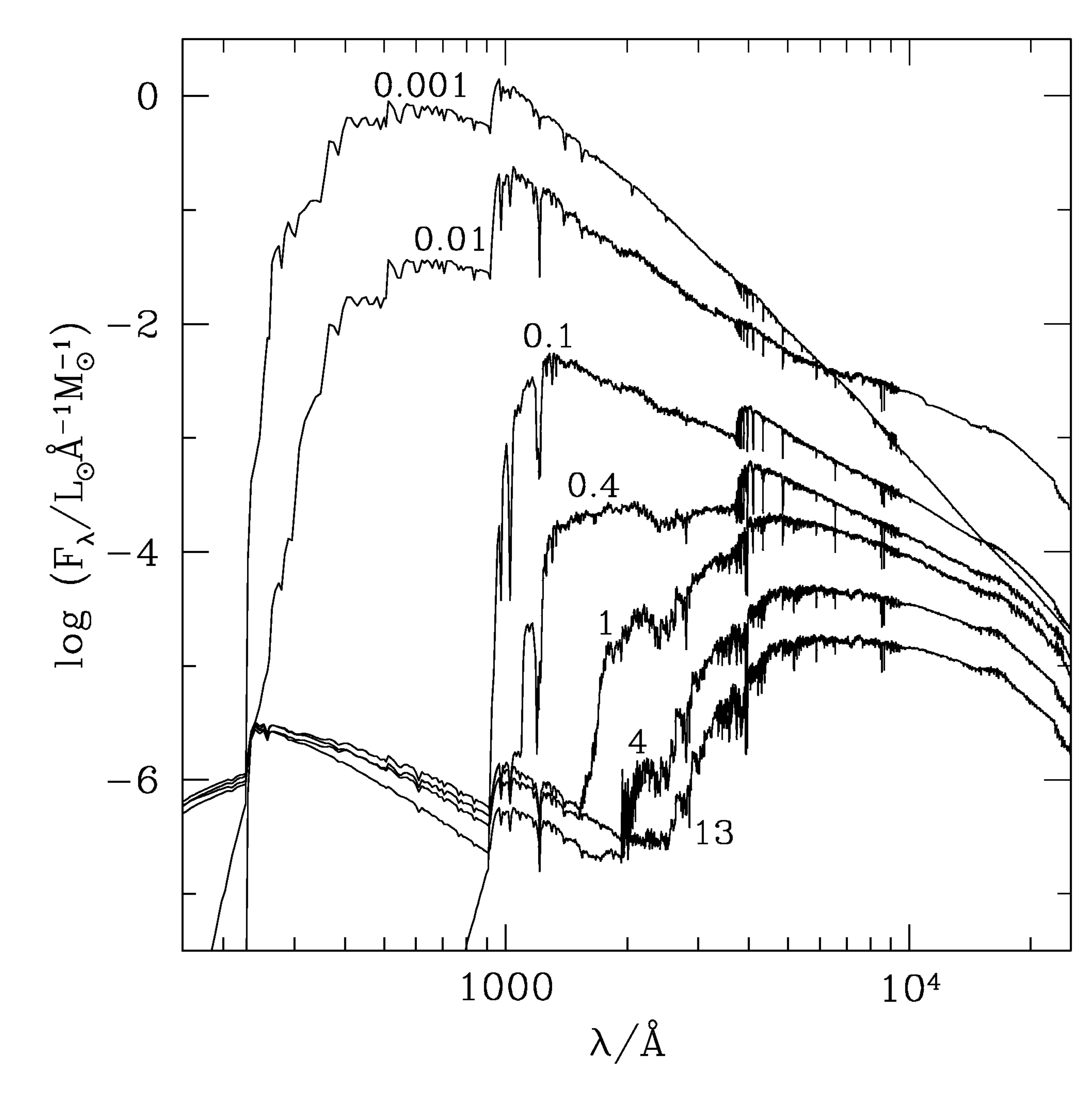

Bruzual & Charlot (2003)

Colour evolution of a SSP

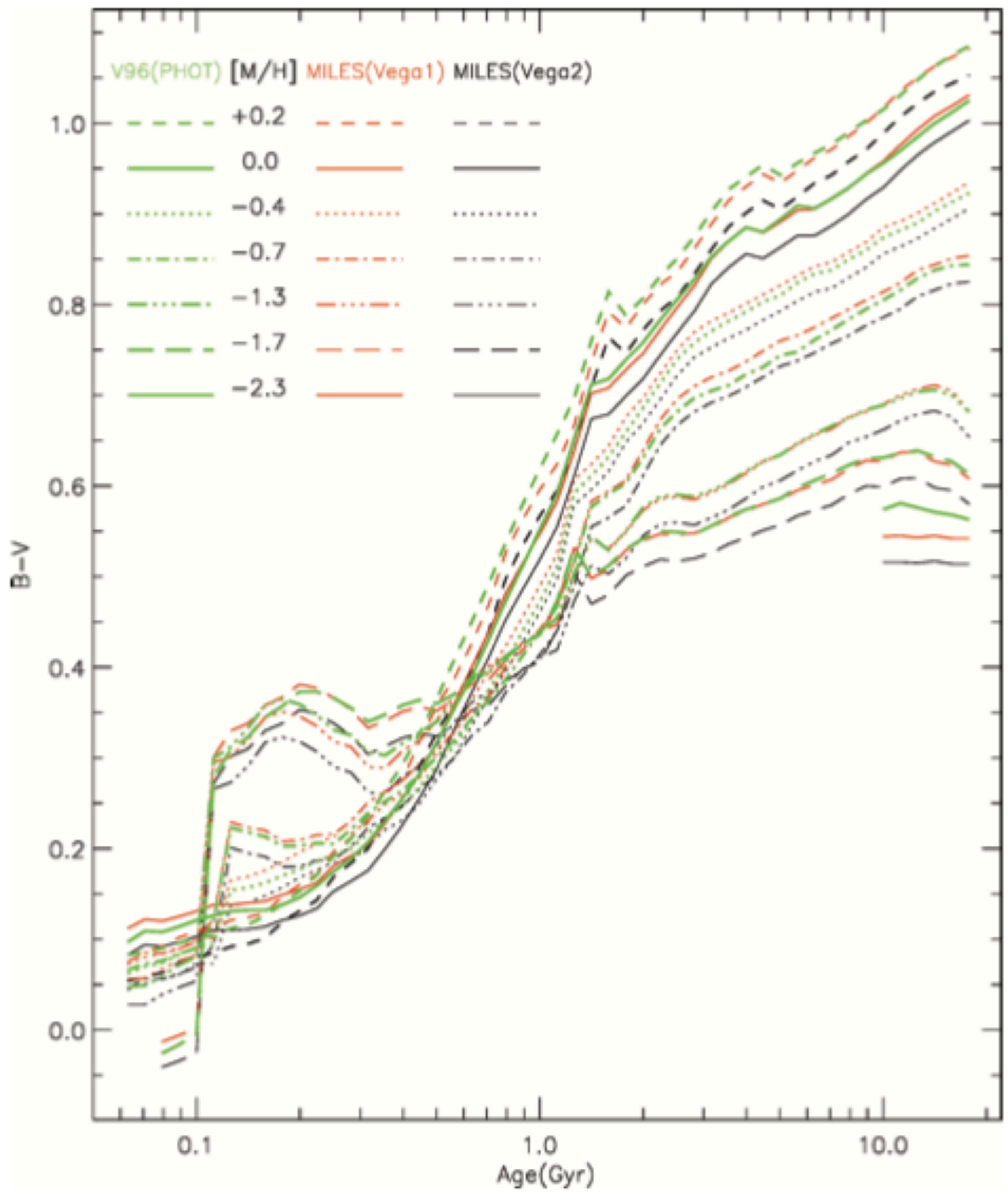

Figure 19. We plot the broad-band $B - V$ colour derived from the SSP SEDs for different ages and metallicities (as indicated within the panel) and the Kroupa universal IMF with the zero-point set with two different Vega spectra in black (very thin) and red (thicker) (see the text for details). The thickest green line represents the photometric colour computed by Vazdekis et al. (1996), as updated in this work, which is based on extensive empirical photometric stellar libraries.

Vazdekis et al. (2010)

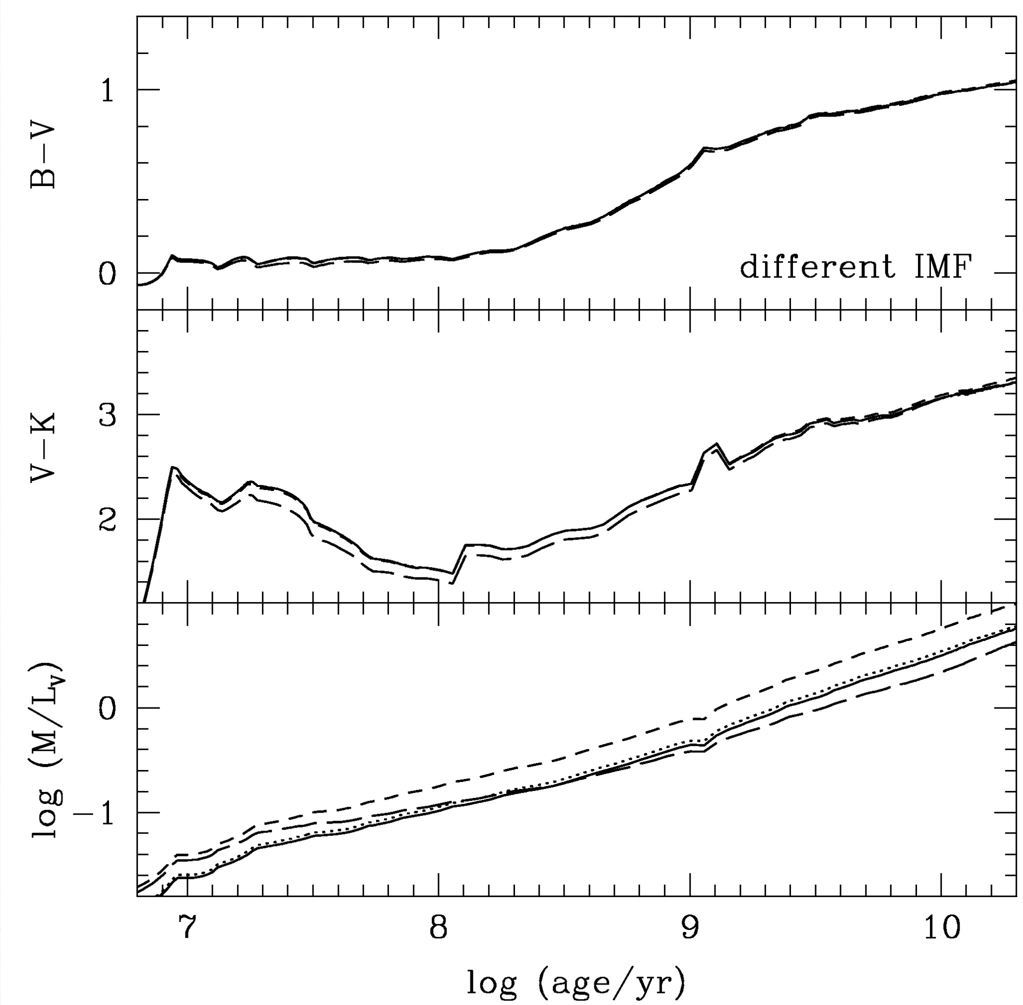

Figure 4. Evolution of the $B - V$ and $V - K$ colours and stellar mass-to-light ratio M/L_V of simple stellar populations of solar metallicity computed using the Padova 1994 stellar evolution prescription and the STELIB/BaSeL 3.1 spectral calibration, for different IMFs: Chabrier (2003b, standard model; solid line; see equation 2), Kroupa (2001, dotted line), Salpeter (1955, short-dashed line) and Scalo (1998, long-dashed line). All IMFs are truncated at 0.1 and 100 $M_\odot$.

Bruzual & Charlot (2003)

Energy budget from different phases

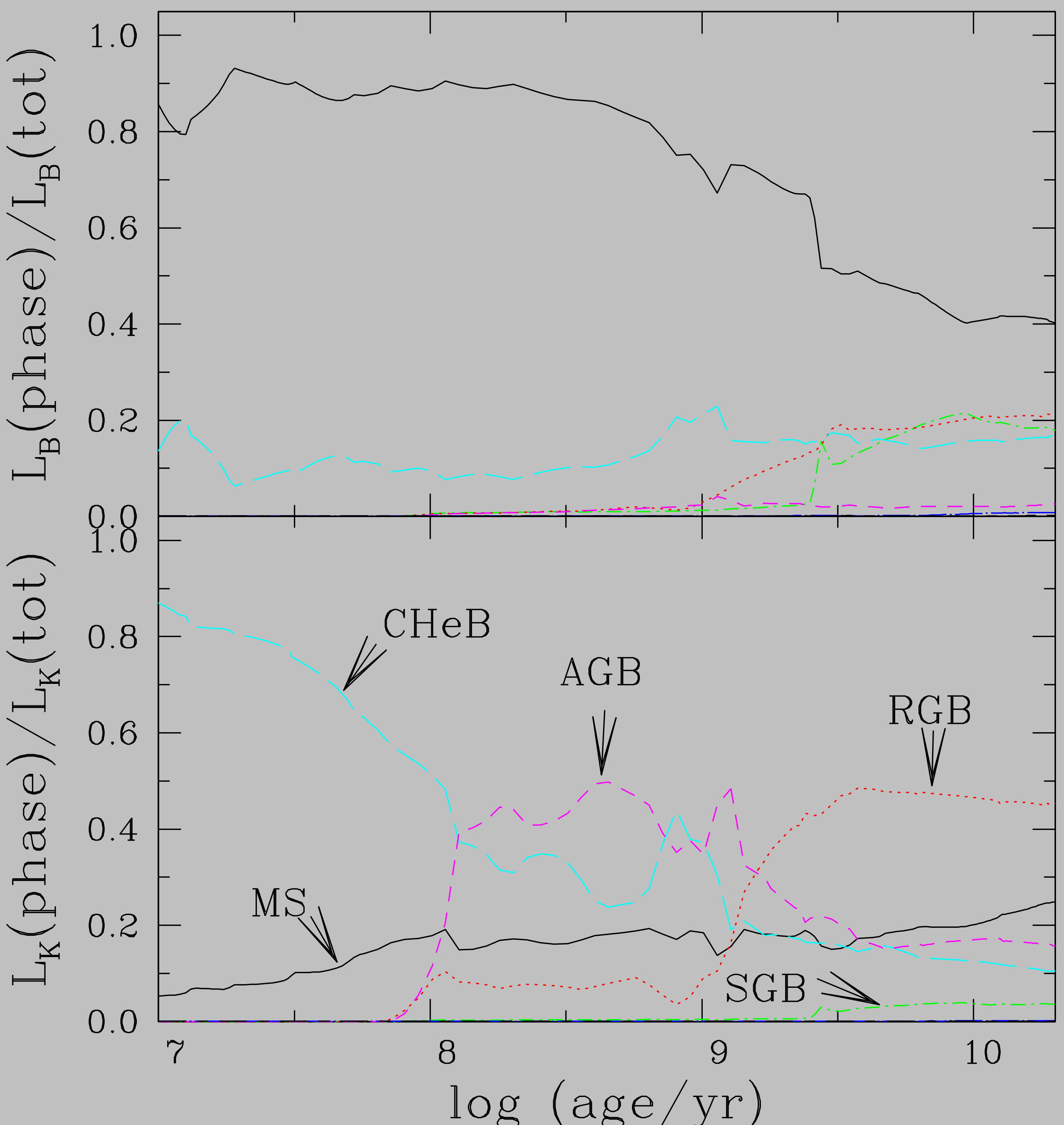

In the optical range the spectrum is always dominated by MS stars. Among them, the most luminous are the ones close to the Turn-Off (TO) point.

Qualitatively, the optical spectrum of a SSP as a function of time is similar to the one of the stars getting off the MS at that time.

In the NIR the main contributors are always cool giant stars, with MS stars never contributing more than 30%

Spectral types and their approximate age at the turn-off

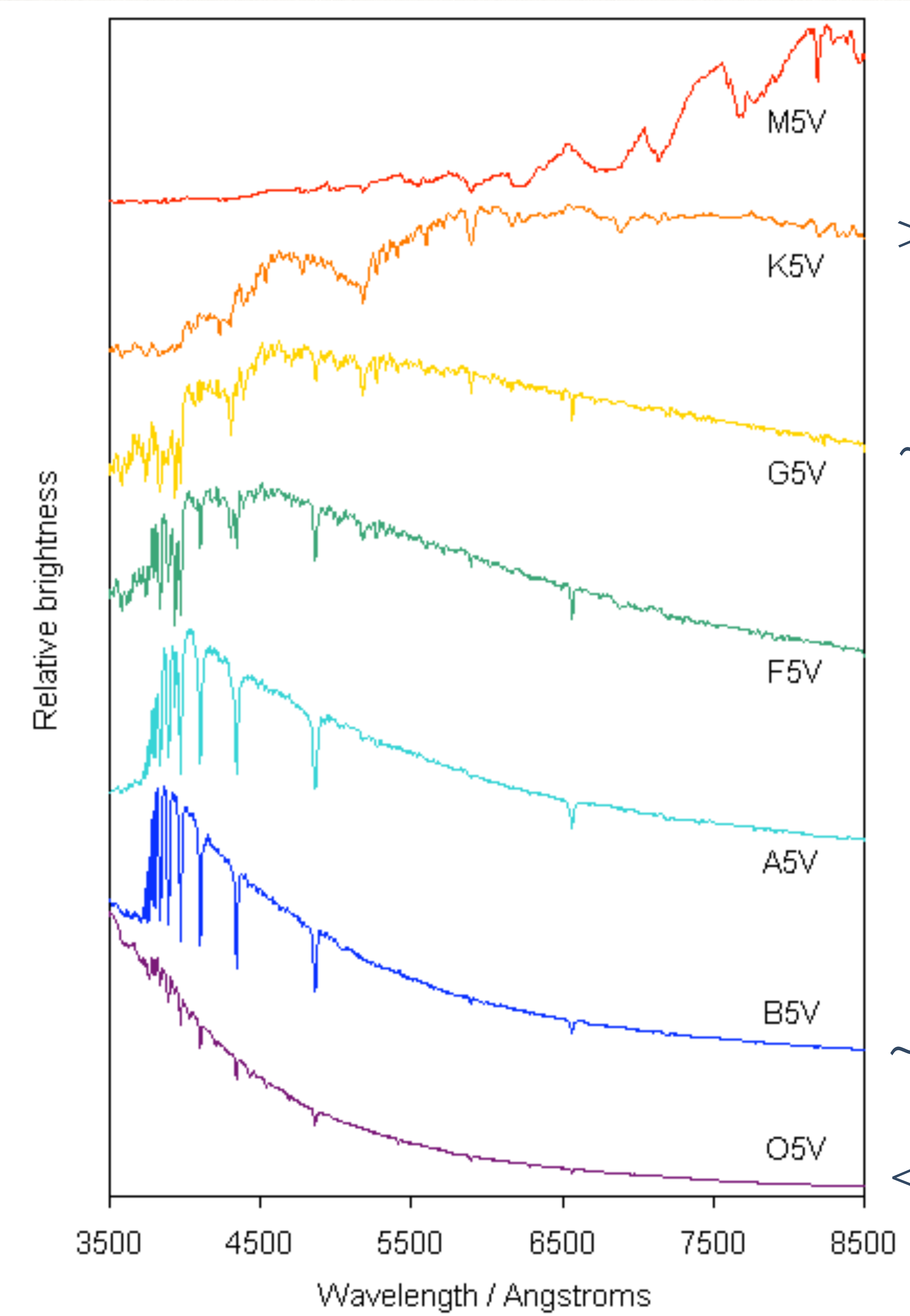

Age(TO)

>12 Gyr

~10 Gyr

~5 Gyr

~1 Gyr

~5 10^7 yr

<~10^7 yr

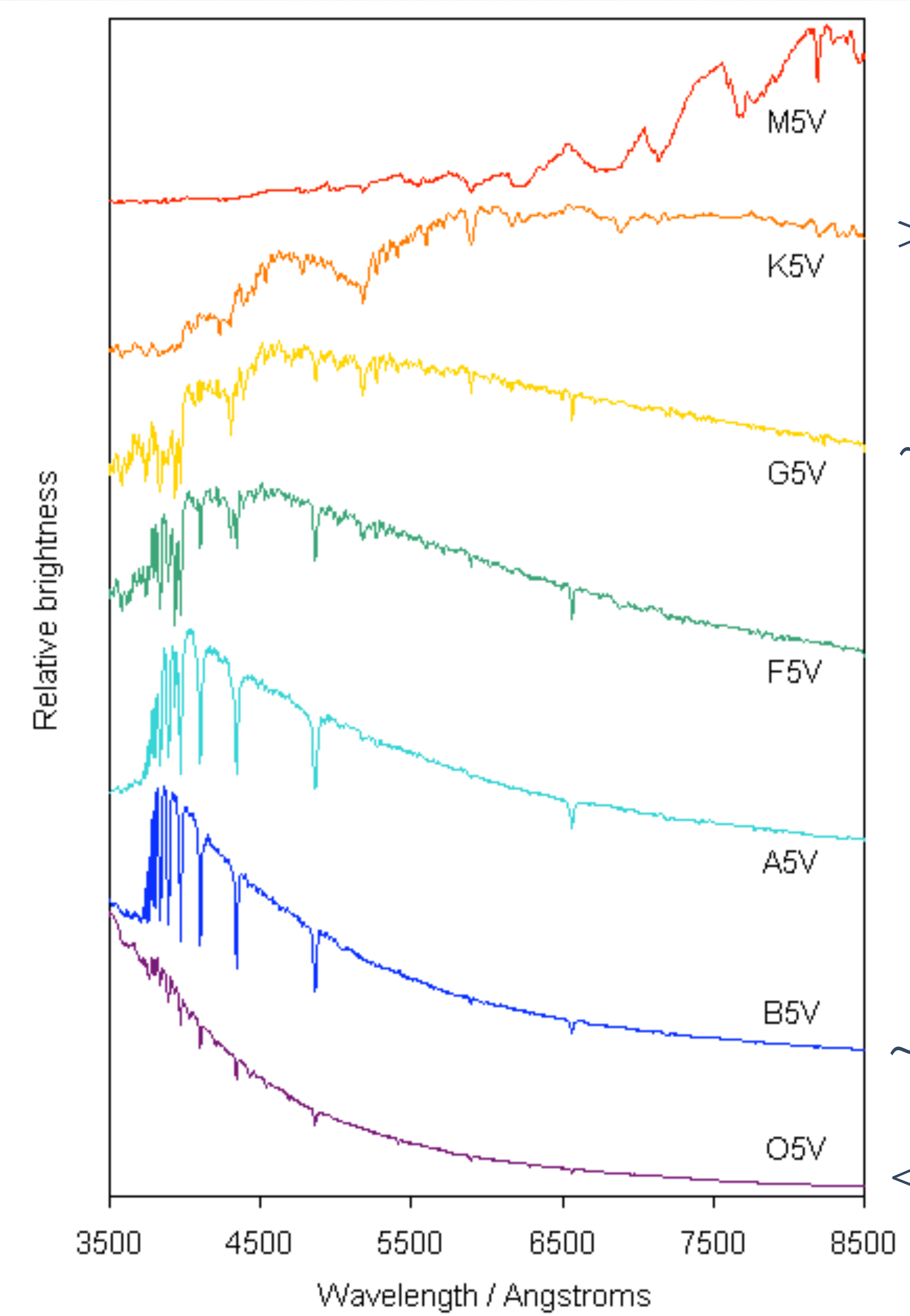

Age(TO)

$>$12 Gyr

$\sim$10 Gyr

$\sim$5 Gyr

$\sim$1 Gyr

$\sim 5\ 10^7$ yr

$<\sim 10^7$ yr

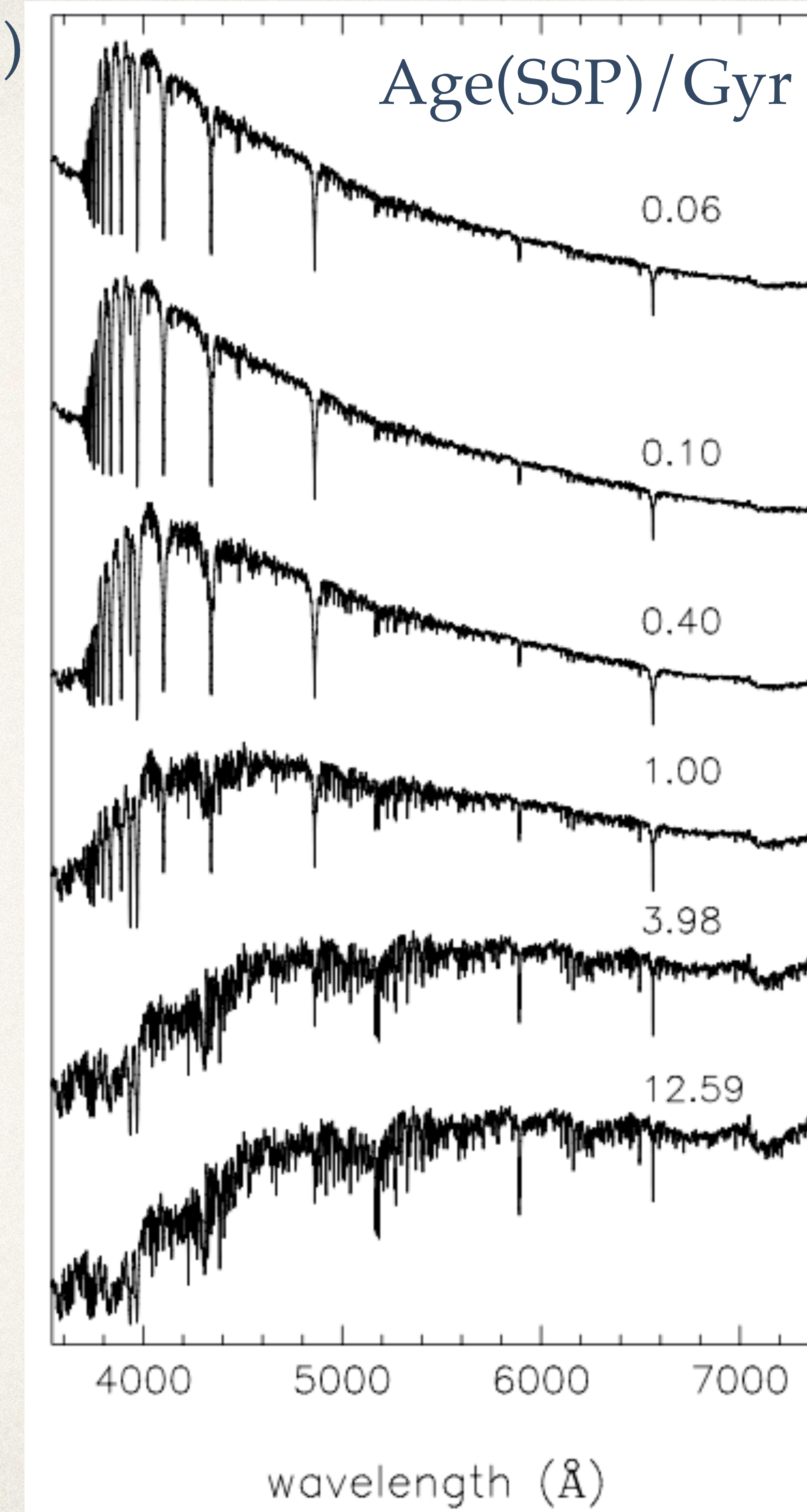

Line strength evolution of an SSP 1. the Balmer lines

- Approximated physical treatment
- Balmer series in absorption: e- excited n=2 → n>2
- Absorption strength proportional to relative abundance of neutral H atoms N_2 in n=2 state to total (neutral atoms in all states + ions)

  $$T_{21} = E_{21}/k = 13.6eV/k(1 - 1/2^2) \sim 1.2 \times 10^5 K$$

  - Approximate $N_{tot} = N^+ + N_1 + N_2 + \ldots \approx N^+ + N_1$
  - Absorption strength ∝ $\approx \dfrac{N_2}{N^+ + N_1}$
- From Boltzmann eqtn. (equilibrium of excited levels) :
- From Saha-Boltzmann eqtns. (equilibrium between ground state and ions):
- Combine:
- ⇒ Strength peaks around a Temperature of the order of the excitation Energy

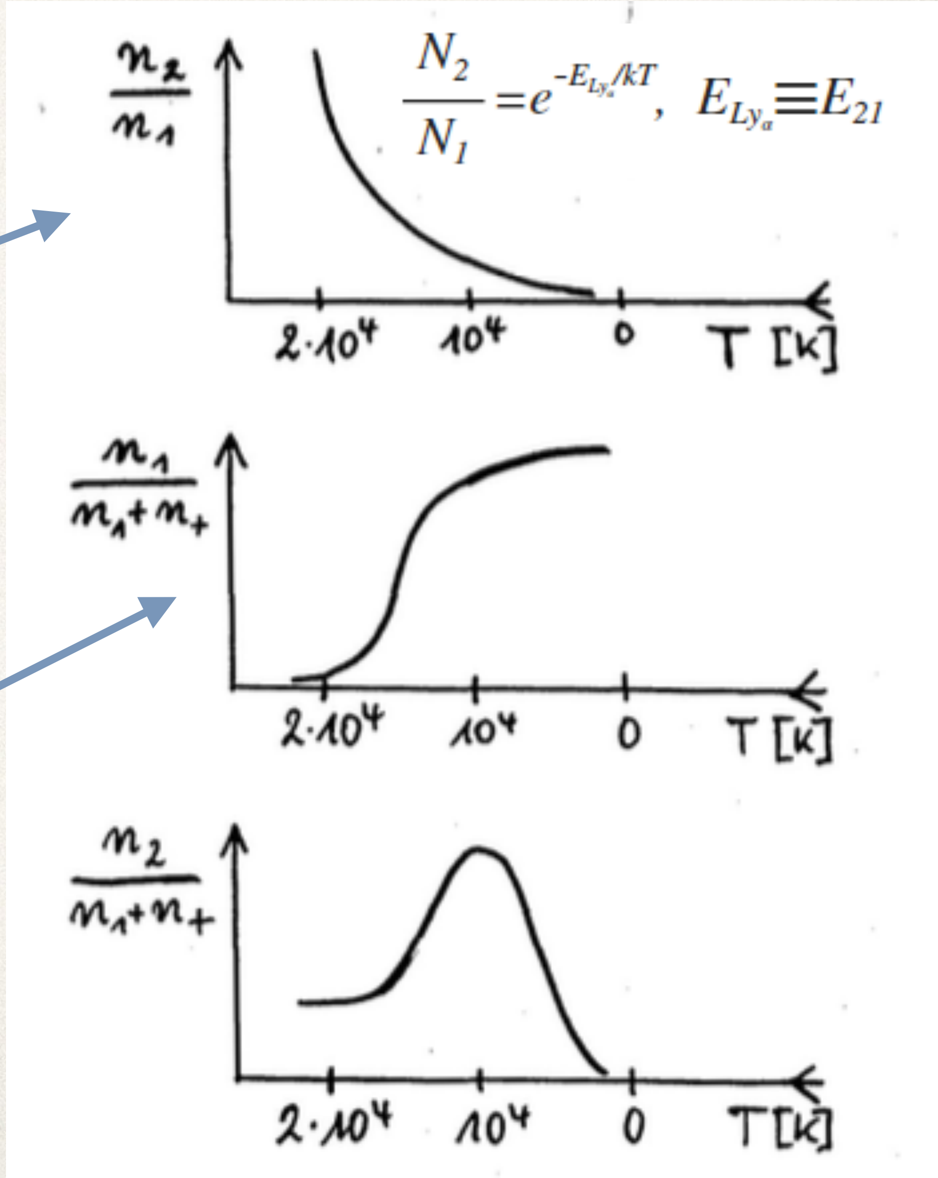

Line strength evolution of an SSP
1. the Balmer lines

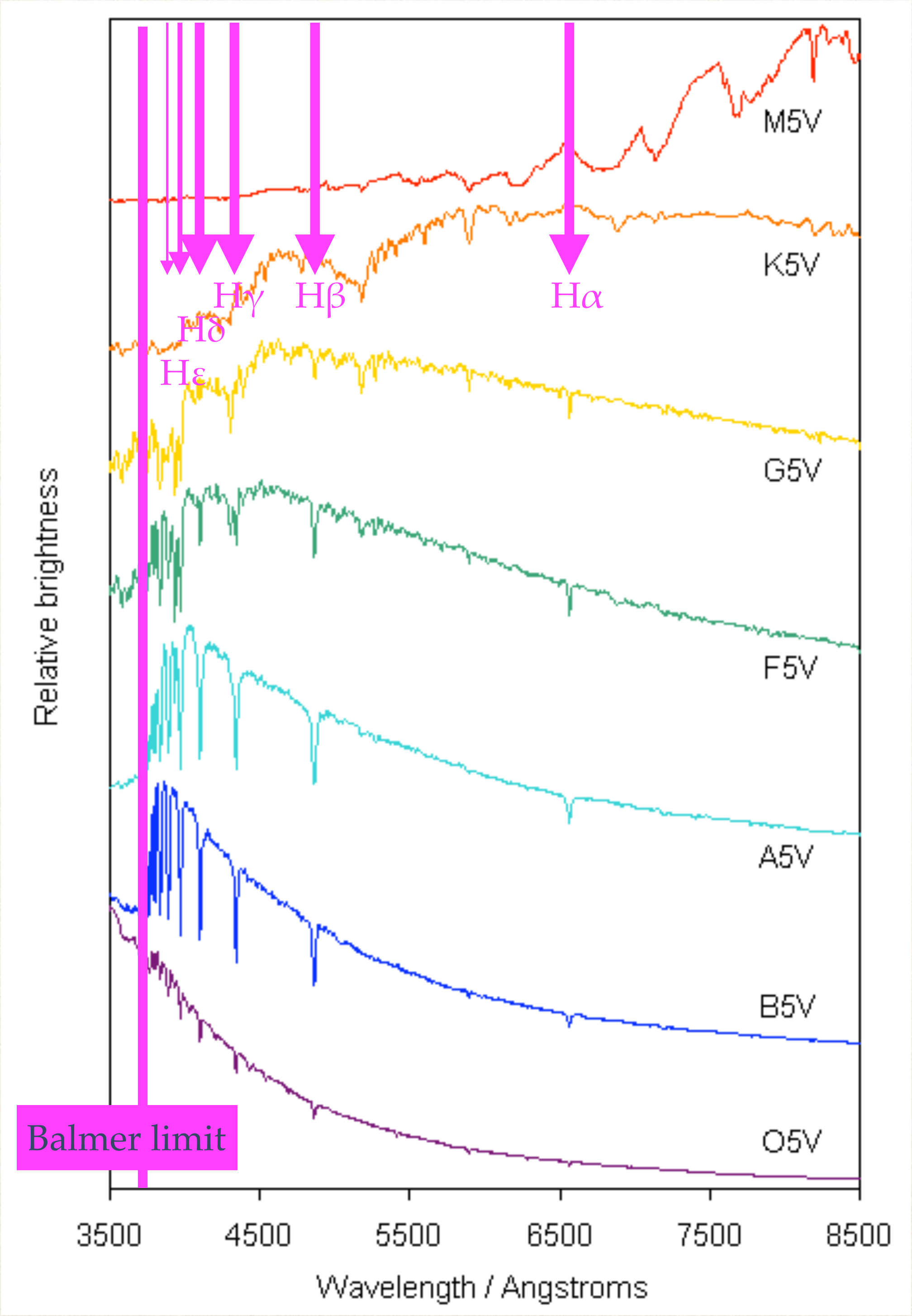

Line strength evolution of an SSP
1. the Balmer lines

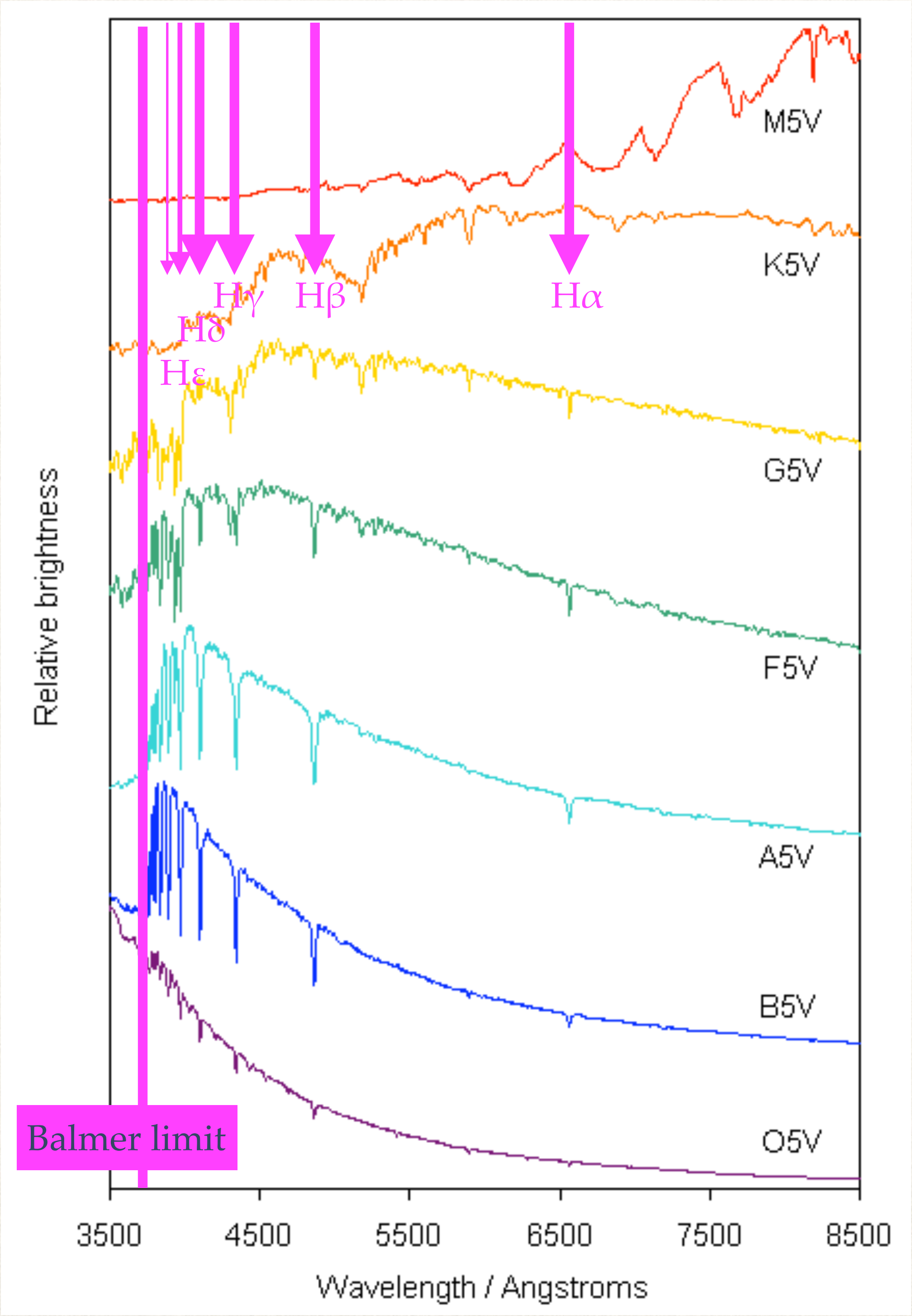

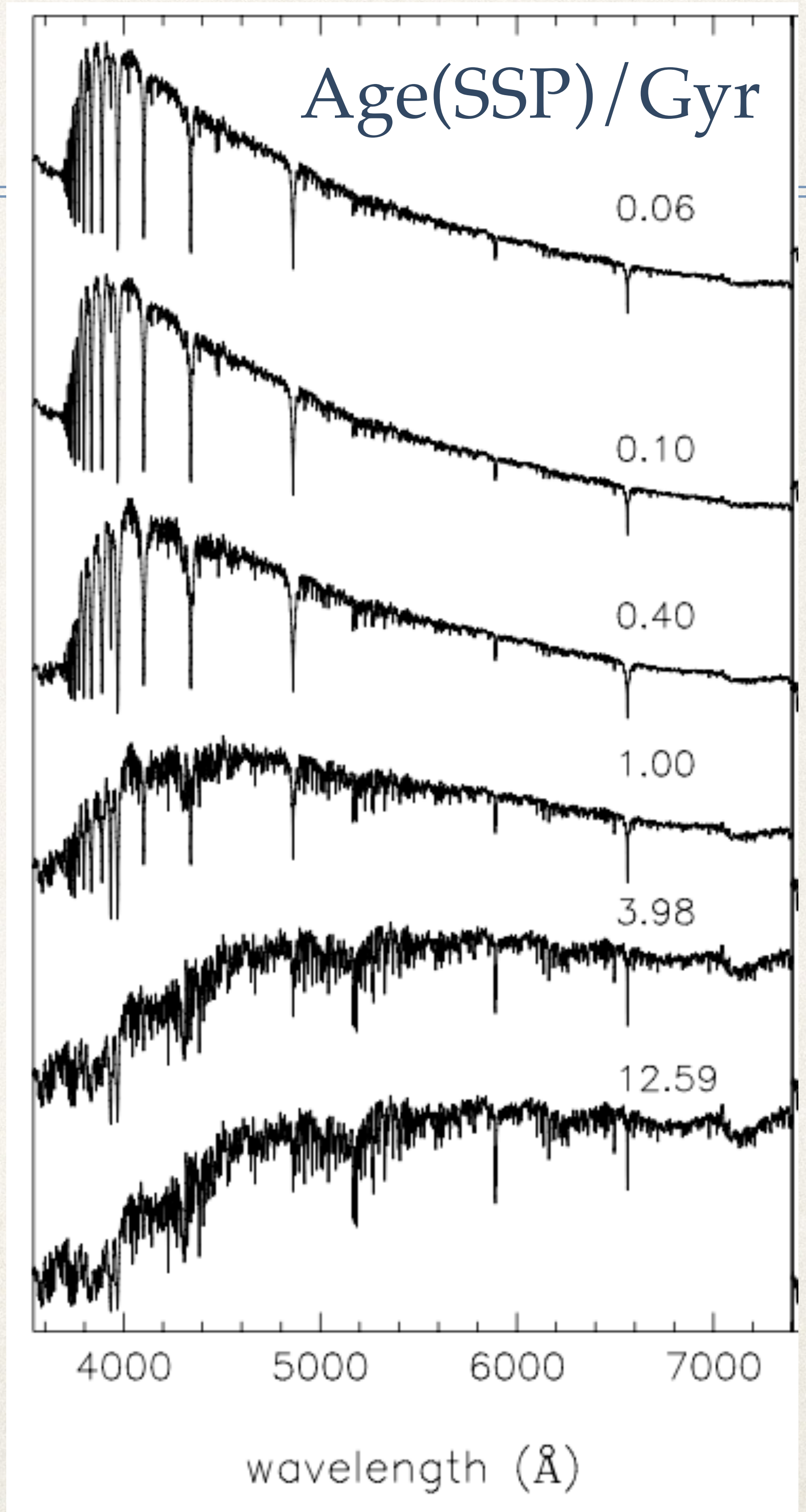

Line strength evolution of an SSP 1. the Balmer lines

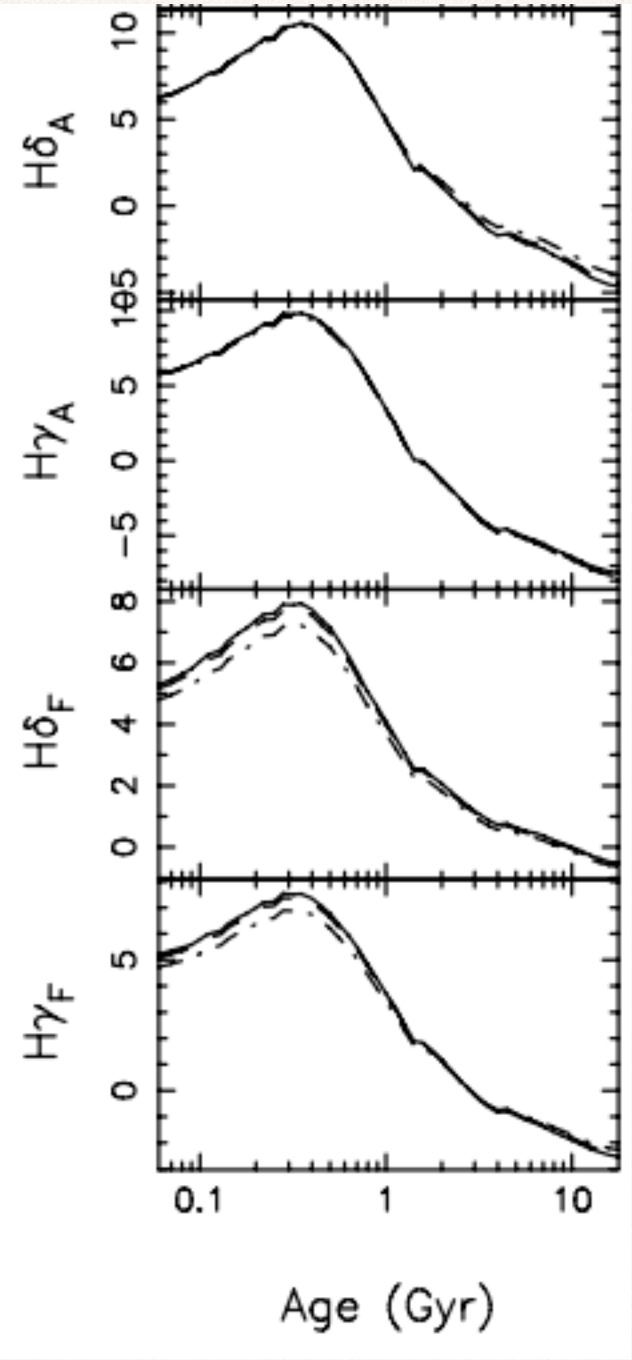

Line strength evolution of an SSP
1. the Balmer lines

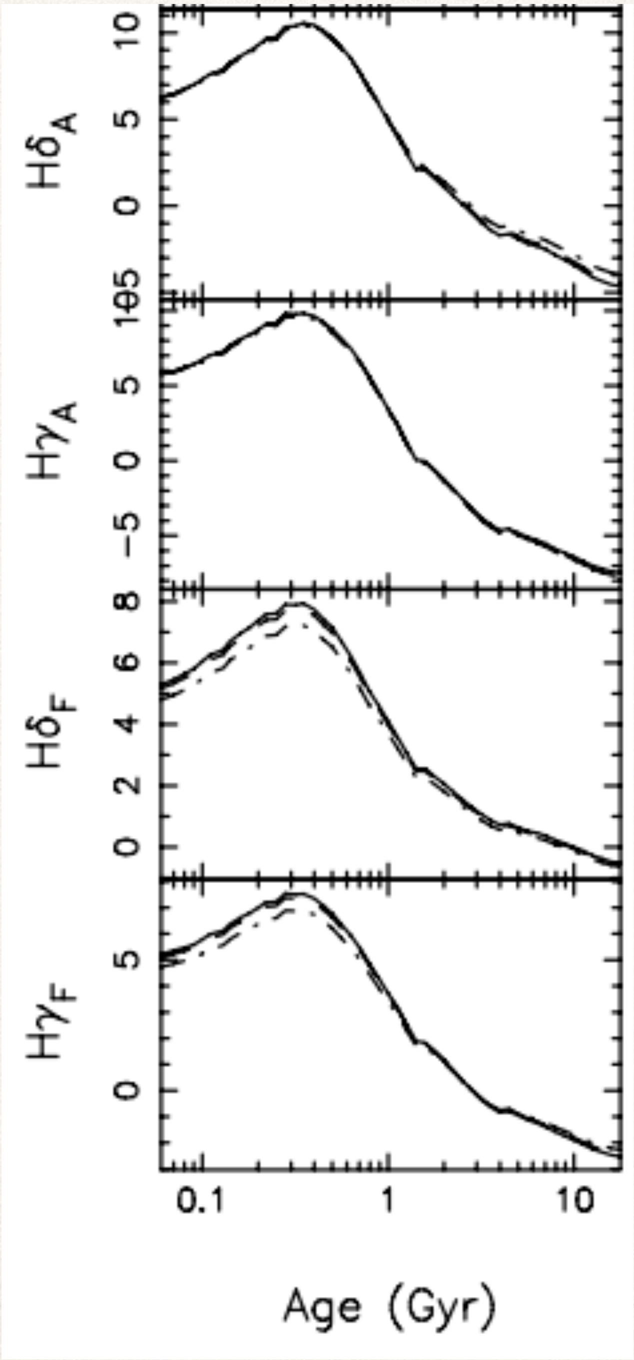

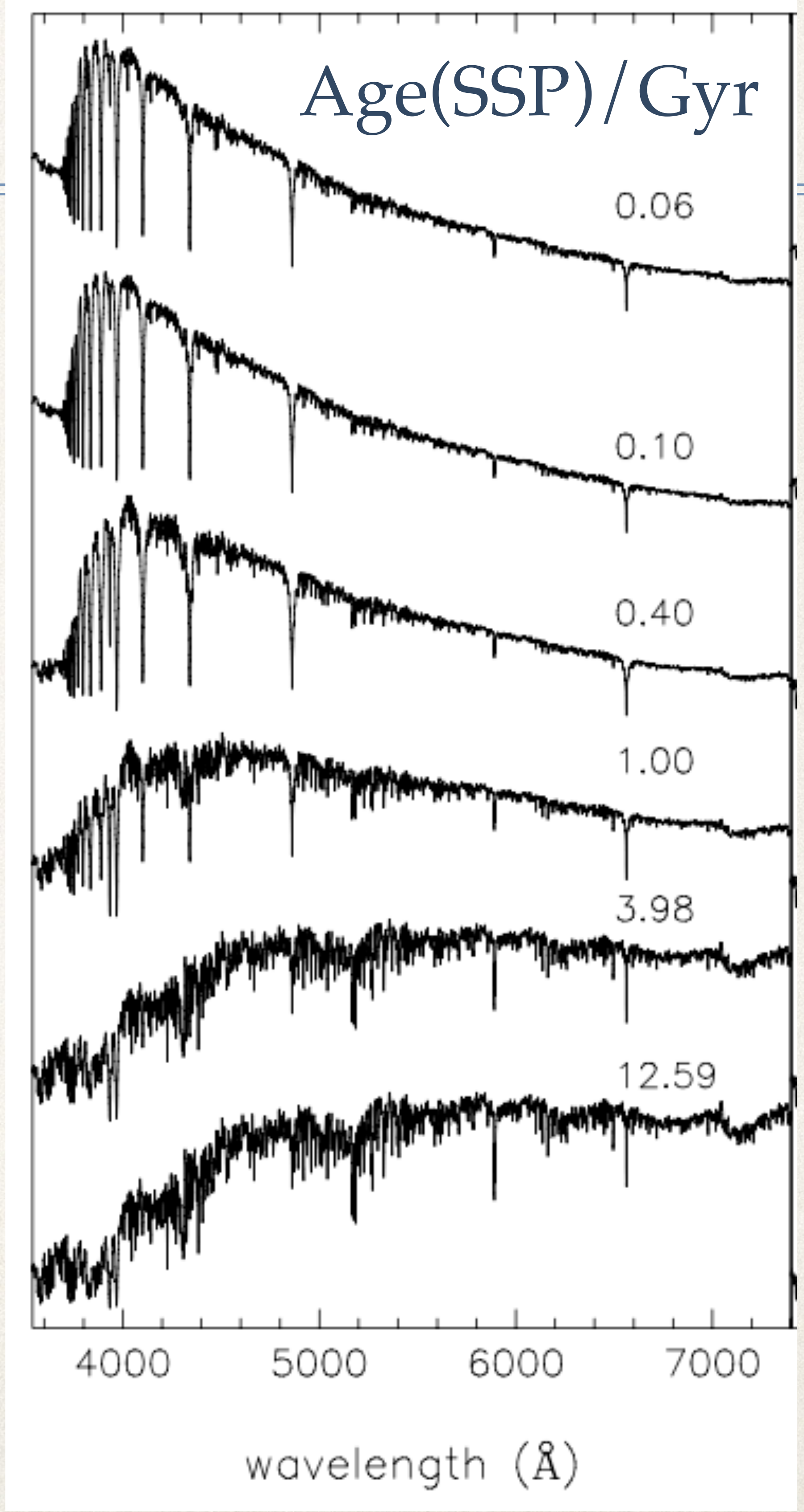

Line strength evolution of an SSP 2. other lines

- Dependence on
  - **Chemical abundance [X/H] (“metallicity”)***
  - <Teff>, which in turn depends on age and metallicity

Variation of absorption lines along the Harvard sequence, i.e. as a function of T_{eff}

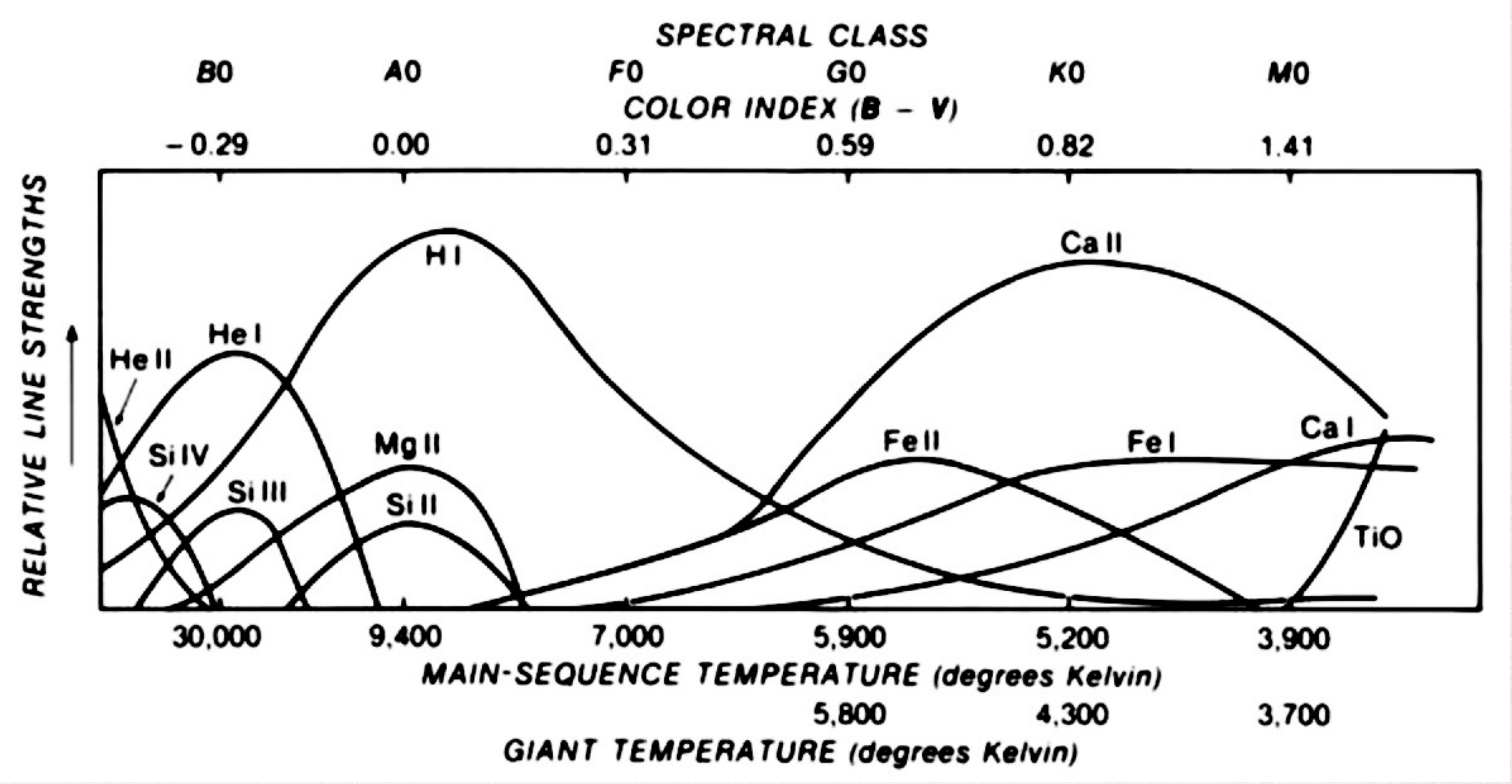

Roman number indicate the ionization stage of the atoms: e.g., H I means neutral hydrogen, He II corresponds to He^{+}, Si III to SI^{++} etc.

* [X/H] denotes the log of abundance of element X with respect to Hydrogen normalised to the same quantity measured in the Solar atmosphere.
* If [X/H] is averaged over all “metals” it can be denoted as [M/H] or $\log(Z/Z_\odot)$ and referred to as “metallicity”

Age dependence of metal indices

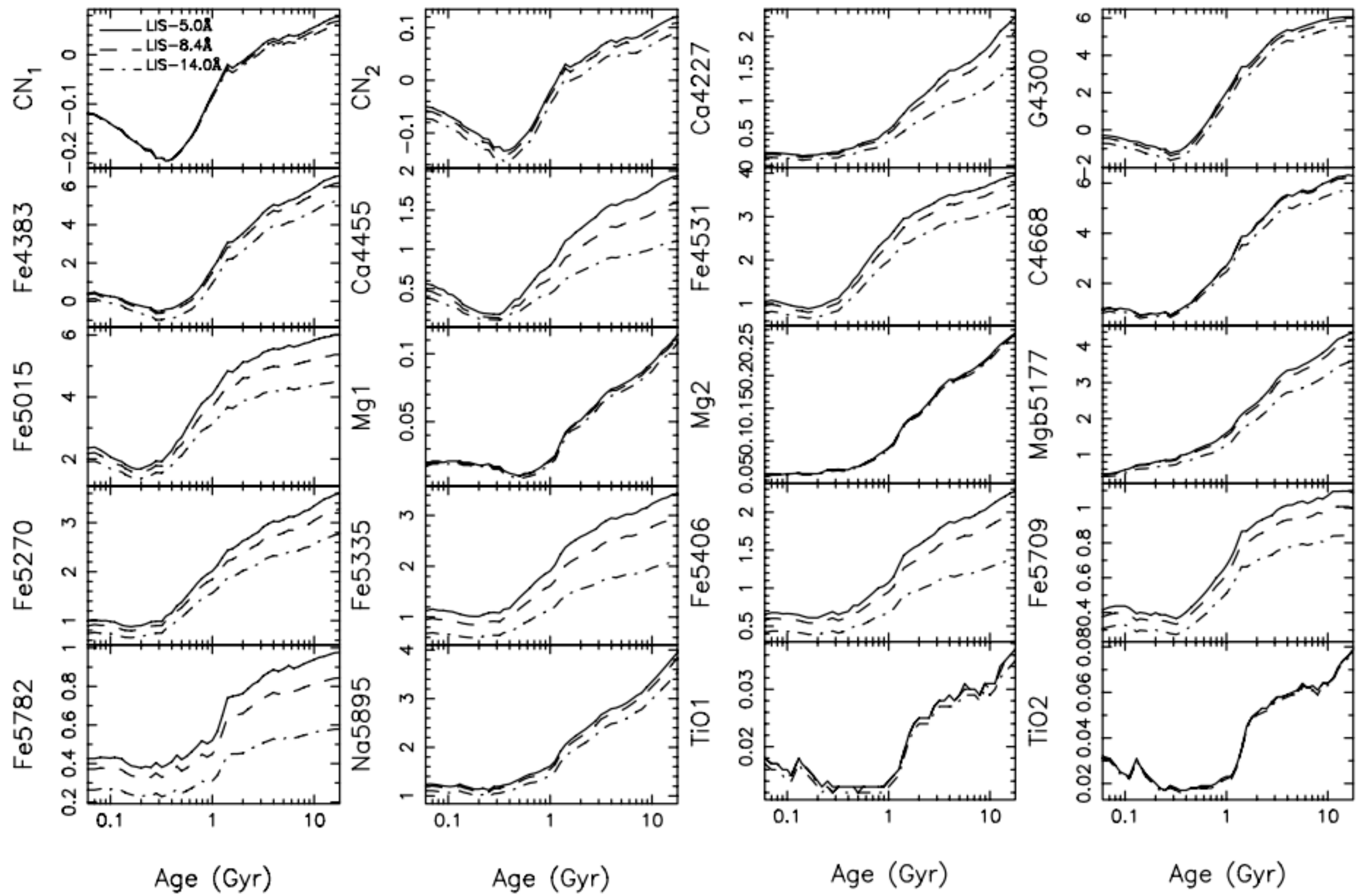

Figure 14. Time evolution of several Lick line-strength indices measured on our new SSP SEDs for solar metallicity and Kroupa universal IMF, smoothed to different resolutions. Solid line: resolution of LIS-5.0 Å (FWHM = 5 Å); dashed line: resolution of LIS-8.4 Å (FHWM = 8.4 Å); dash–dotted line: resolution of LIS-14.0 Å (FWHM = 14 Å).

Vazdekis et al. (2010)

Balmer break / D4000 break

- Balmer-series limit combined with many metal absorptions
- Monotonic age indicator
- Affected by metallicity as well

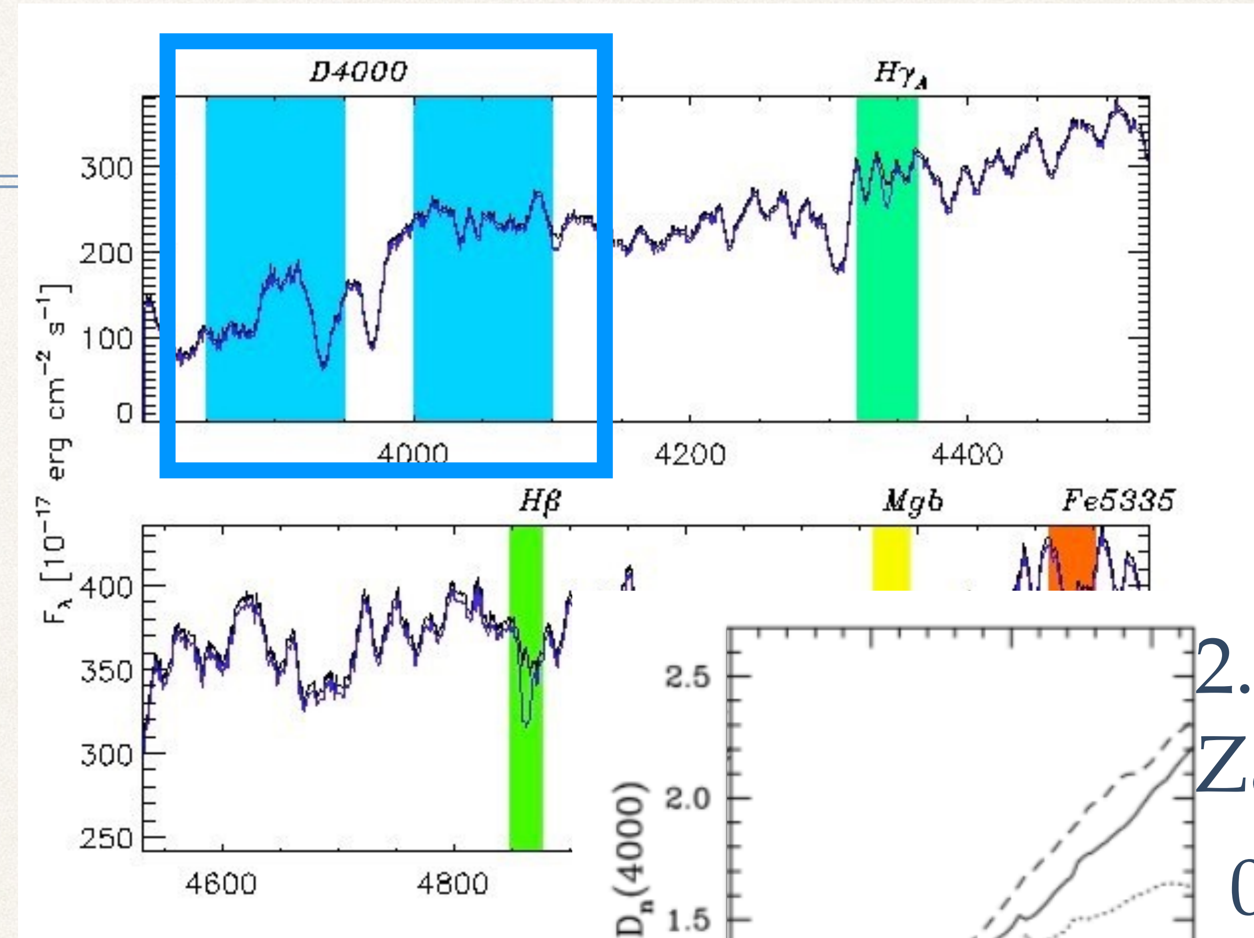

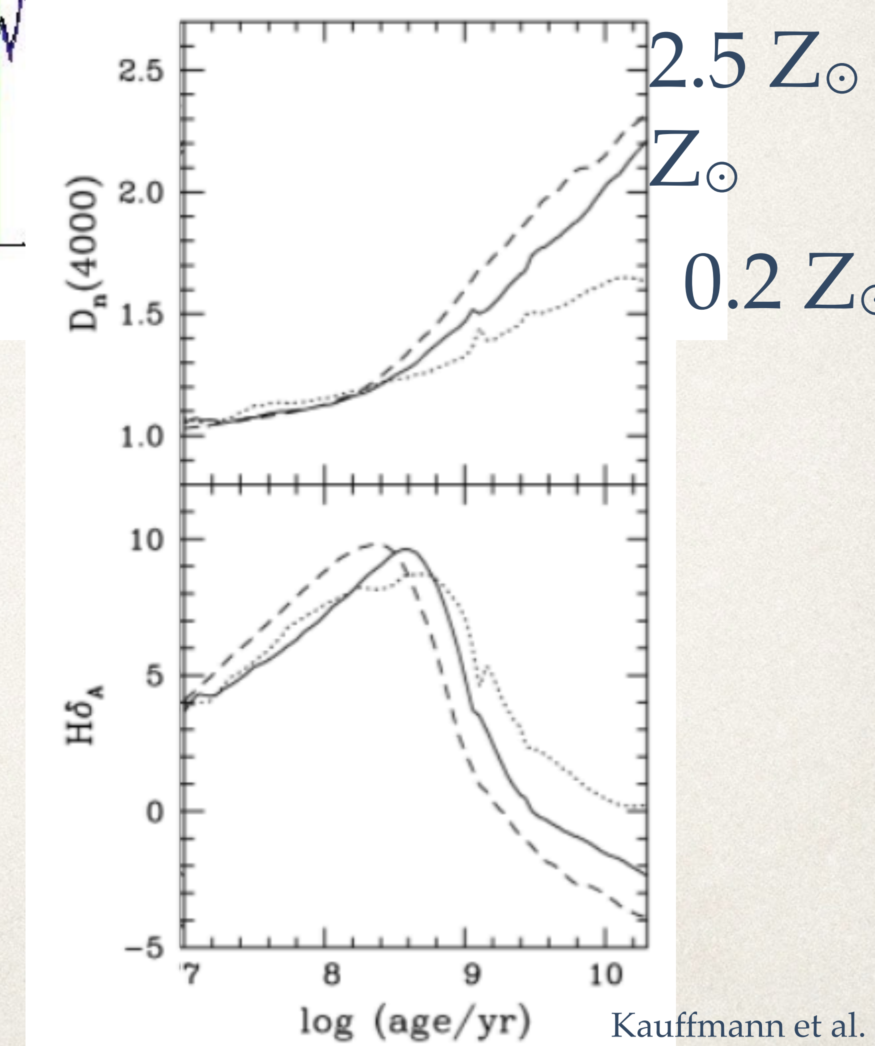

Kauffmann et al. (2003)

Line strength evolution of an SSP
3. index grids

- No spectral index is pure age nor pure metallicity indicator
- Combine indices in grids
- Find a combination that is as much “orthogonal” as possible

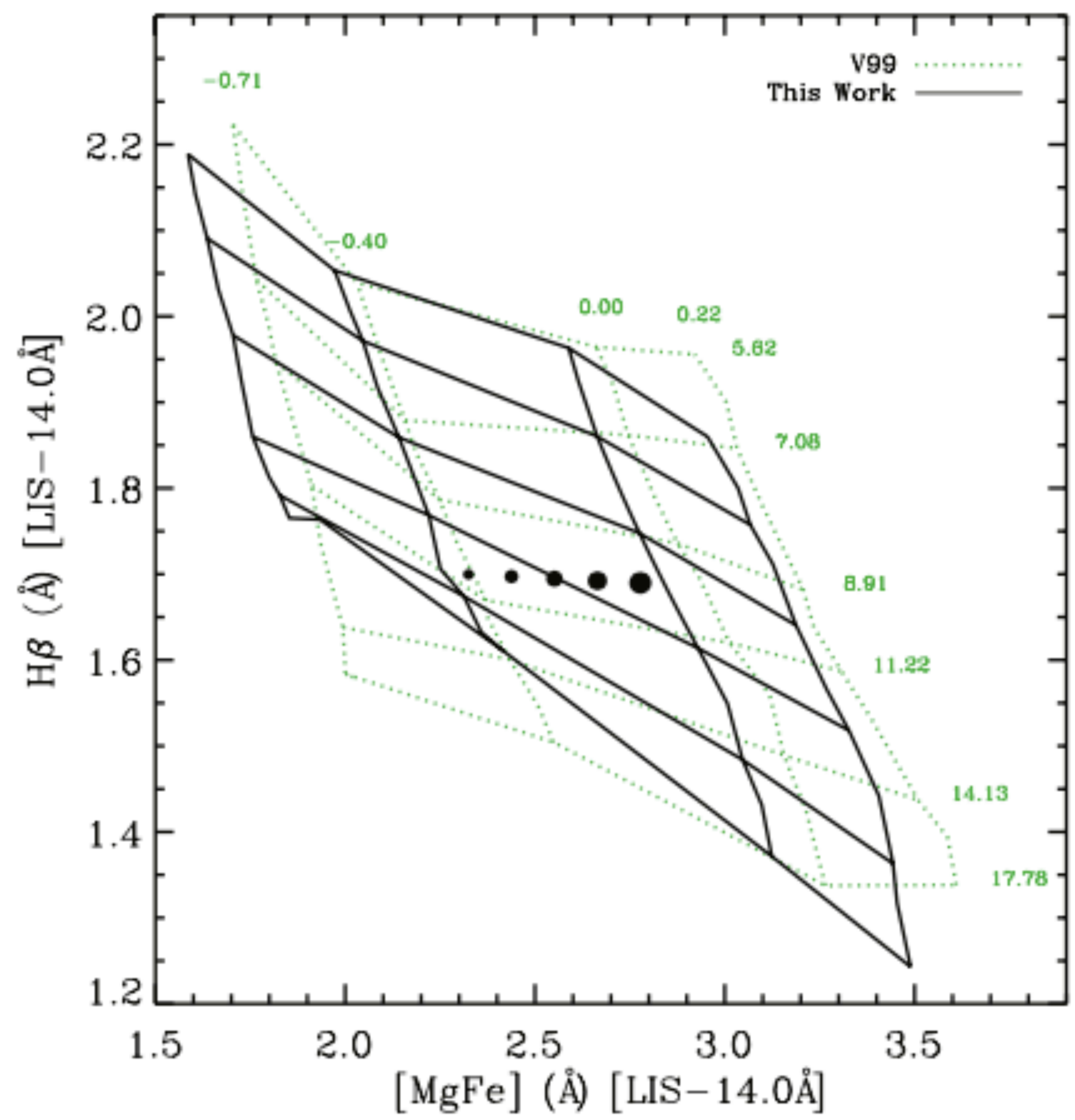

Figure 26. Hβ versus [MgFe] diagnostic diagram obtained from our MILES base model SEDs (solid line) and V99 (dotted line), which uses the Jones (1999) stellar library. The indices were measured on the SSP spectra once smoothed to match the LIS-14.0 Å resolution. We plot the radial line-strength profile for the Virgo galaxy NGC 4387, which has been obtained from low-resolution Keck/LRIS spectra by Sánchez-Blázquez et al. (2007). The size of the filled circles decreases with an increasing galactocentric distance: 1.25, 2.5, 5, 10 and 20 arcsec.

Vazdekis et al. (2010)

Dust: extinction vs attenuation

- Extinction measures the total loss of light along a single line of sight: absorption + off-scatter
- Attenuation:
  - light can be scattered both out of and into a given line of sight
  - the geometrical distribution of dust with respect to the stars strongly affects the resulting SED

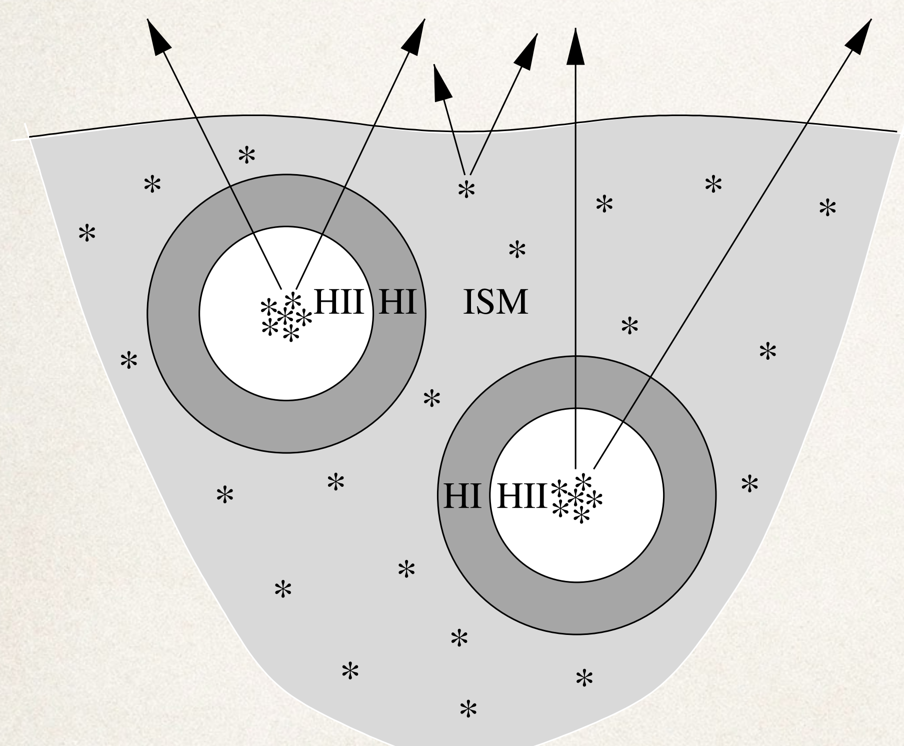

FIG. 1.—Schematic representation of the birth cloud and ambient ISM surrounding each generation of stars in a model galaxy (see text). Rays leaving in different directions are also shown.

Extinction curves

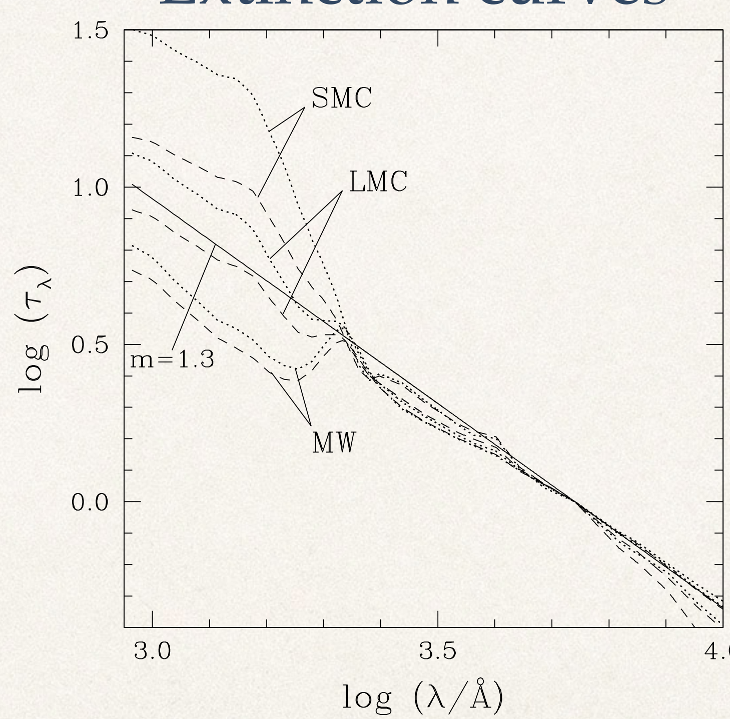

FIG. 9.—Optical depth of graphite-silicates dust plotted against wavelength. The dotted lines are the true absorption curves of the Milky Way, LMC, and SMC, while the dashed lines are the corresponding curves when isotropic scattering is included (eq. [19]). These are based on the Draine & Lee (1984) model but with the proportions of graphite and silicates adjusted so as to fit the observed mean extinction curves of the three galaxies (Pei 1992). The solid line is a power law of index $m = 1.3$. All curves are normalized to unity at 5500 Å.

Effective attenuation curves

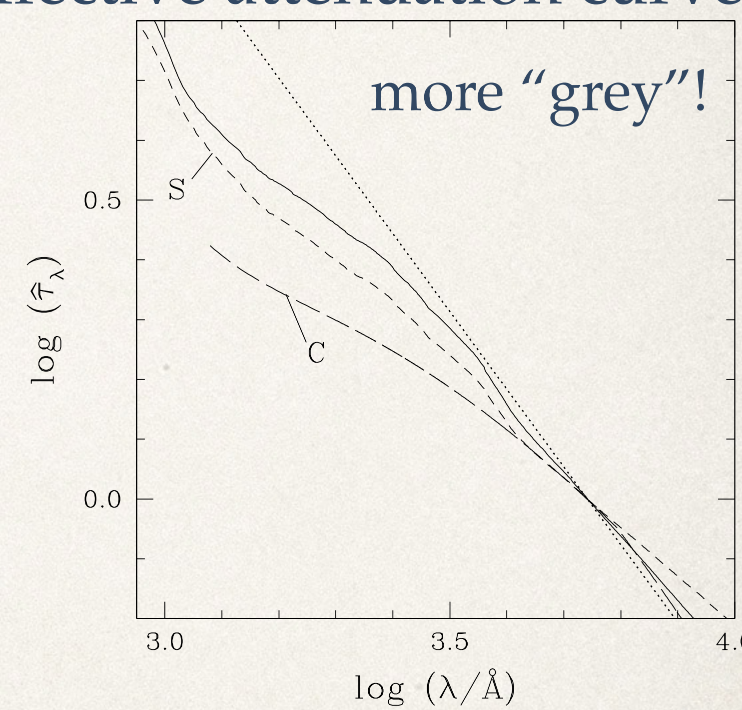

FIG. 10.—Effective absorption curve (as defined by eq. [4]) of a model with effective starburst age $t = 3 \times 10^8$ yr in which the ambient ISM is represented by a mixed slab (*solid line*). The optical depth of the dust is assumed to have the form $\tau_\lambda \propto \lambda^{-m}$ with $m = 1.3$ (*dotted line*). The short-dashed curve is the standard model of eq. (30), and the long-dashed curve is from Calzetti et al. (1994). All curves are normalized to unity at 5500 Å.

Charlot & Fall (2000); see Chevallard et al. (2013) for updated modeling

Dust "the hard way": radiative transfer codes

- **Trace** the scattering, absorption and re-emission of photons in realistic distributions of dust and stars
  - TRADING (Bianchi 2008)
  - GRASIL (Silva et al. 1998)
  - SUNRISE (Johnson 2006)
  - SKIRT (Baes & Dejonghe 2002)
  - Tuffs & Popescu
  - ….

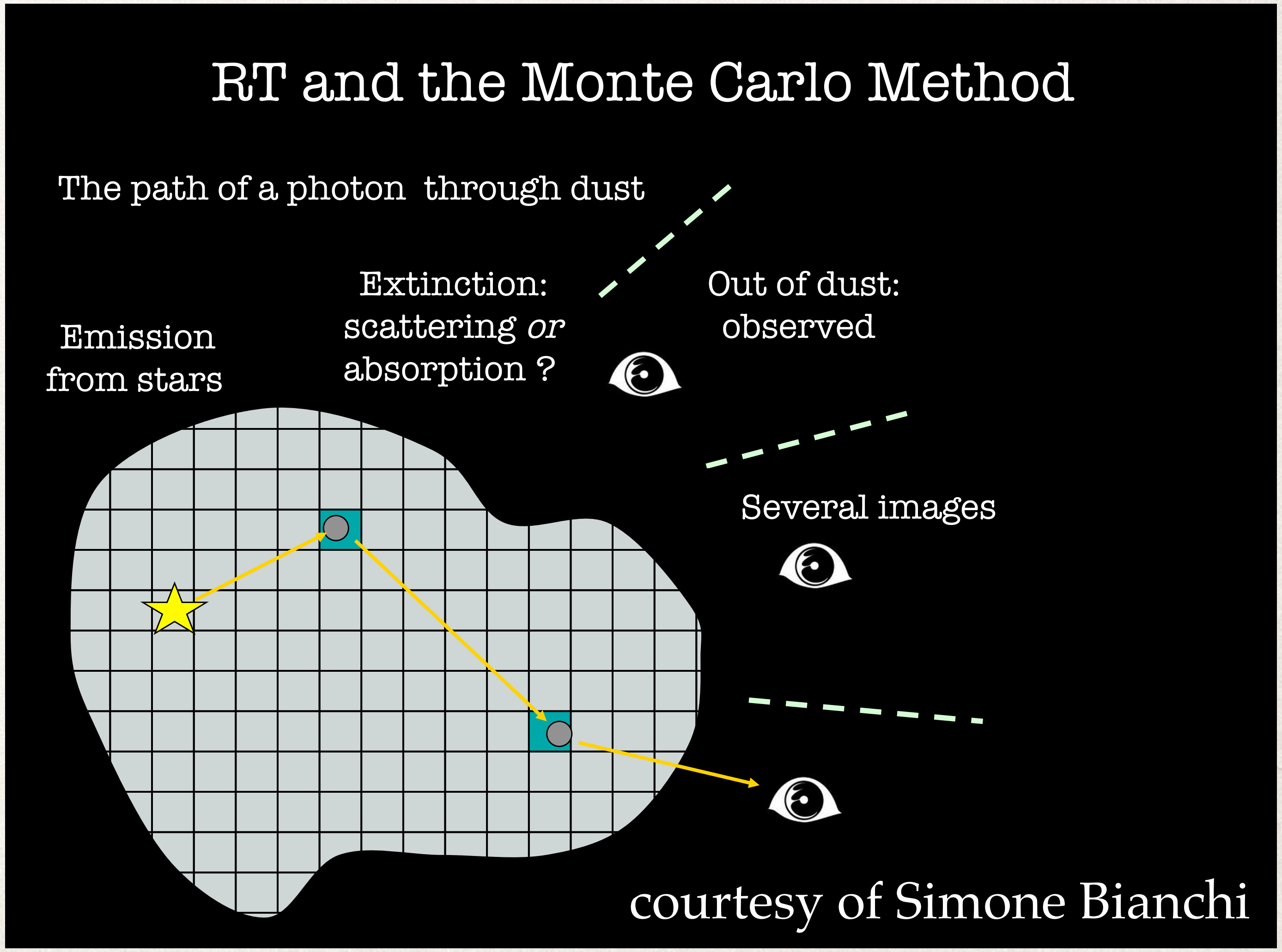

courtesy of Simone Bianchi

Real galaxies vs models

NGC 5746

+ 6 other objects
Bianchi (2007)

V band

model

K' band

model